Renewable Energy 125 (2018) 630–647

Contents lists available at ScienceDirect

Renewable Energy

journal homepage: www.elsevier.com/locate/renene

The influence of waves on morphodynamic impacts of energy extraction at a tidal stream turbine site in the Pentland Firth

I. Fairley*, H. Karunarathna, I. Masters

Energy and Environment Research Group, ESRI, College of Engineering, Swansea University Bay Campus, Fabian Way, Swansea, SA1 8EN, UK

ARTICLE INFO

Article history:
Received 1 January 2017
Received in revised form
8 December 2017
Accepted 6 February 2018
Available online 7 February 2018

Keywords:
Tidal stream turbines
Environmental impact assessment
Waves
Morphodynamics
Numerical modelling
Pentland firth

ABSTRACT

Extraction of energy from tidal streams has the potential to impact on the morphodynamics of areas such as sub-tidal sandbanks via alteration of hydrodynamics. Marine sediment transport is forced by both wave and tidal currents. Past work on tidal stream turbine impacts has largely ignored the contribution of waves. Here, a fully coupled hydrodynamic, spectral wave and sediment transport model is used to assess the importance of including waves in simulations of turbine impact on seabed morphodynamics. Assessment of this is important due to the additional expense of including waves in simulations. Focus is given to a sandbank in the Inner Sound of the Pentland Firth. It is found that inclusion of wave action alters hydrodynamics, although extent of alteration is dependant of wave direction. Magnitude of sediment transport is increased when waves are included in the simulations and this has implications for morphological and volumetric changes. Volumetric changes are substantially increased when wave action is included: the impact of including waves is greater than the impact of including tidal stream turbines. Therefore it is recommended that at tidal turbine array sites exposed to large swell or wind-seas, waves should be considered for inclusion in simulations of physical impact.

© 2018 The Authors. Published by Elsevier Ltd. This is an open access article under the CC BY license (http://creativecommons.org/licenses/by/4.0/).

1. Introduction

Tidal stream turbines (TSTs) are maturing as a means of renewable energy generation: several demonstration devices have been deployed and the world's first array will be installed in the Inner Sound of the Pentland Firth with the aim of 386 MW of installed capacity by 2020 [1]; [2]. Presence of support structures and extraction of energy will impact a range of receptors, both physical [3–7] and biological [8–11]. This contribution simulates impact to the morphodynamics of sub-tidal sandbanks using a fully coupled wave – hydrodynamic - sediment transport model. This enables inclusion of wave driven sediment transport and wave-current interaction (WCI) in the computation. Attention is given to a sandbank in the Inner Sound of the Pentland Firth (Fig. 1), close to the Meygen Inner Sound array site [2].

Sub-tidal sandbanks must be considered in environmental impact assessments because they can be important ecological habitats, navigational hazards and sources of aggregates. A substantial amount of work has been conducted on the physical processes governing the morphology of sub-tidal sandbanks [12–16]. Sandbanks are often formed and maintained by residual current gyres which are caused by tidal asymmetry around headlands. Sub-tidal sandbanks can be found in the centre of these circulation patterns. The importance of the contribution of waves to sandbank morphodynamics and long term evolution is open to debate [17]. Dependant on environmental setting, the background stirring influence of low energy waves may be important [18] or episodic storm events may be more relevant [19,20]. Under storm conditions, tidal residuals may be reversed [21,22] both due to WCI and the dominance of wave driven currents.

The process of WCI is complex and highly studied phenomenon with both waves affecting currents and currents affecting waves (e.g. Refs. [23,24]). When waves propagate in a current field, various phenomena can occur, including: altered wind wave growth; current induced refraction; changes to wave steepness which alters rates of dissipation [25]; and wave blocking. Wave blocking is the prevention of wave energy transport caused when current velocity is equal and opposite to the wave group velocity [26,27]. The presence of waves can alter currents via two main

* Corresponding author.
E-mail addresses: i.a.fairley@swansea.ac.uk (I. Fairley), h.u.karunarathna@swansea.ac.uk (H. Karunarathna), i.masters@swansea.ac.uk (I. Masters).

https://doi.org/10.1016/j.renene.2018.02.035
0960-1481/© 2018 The Authors. Published by Elsevier Ltd. This is an open access article under the CC BY license (http://creativecommons.org/licenses/by/4.0/).

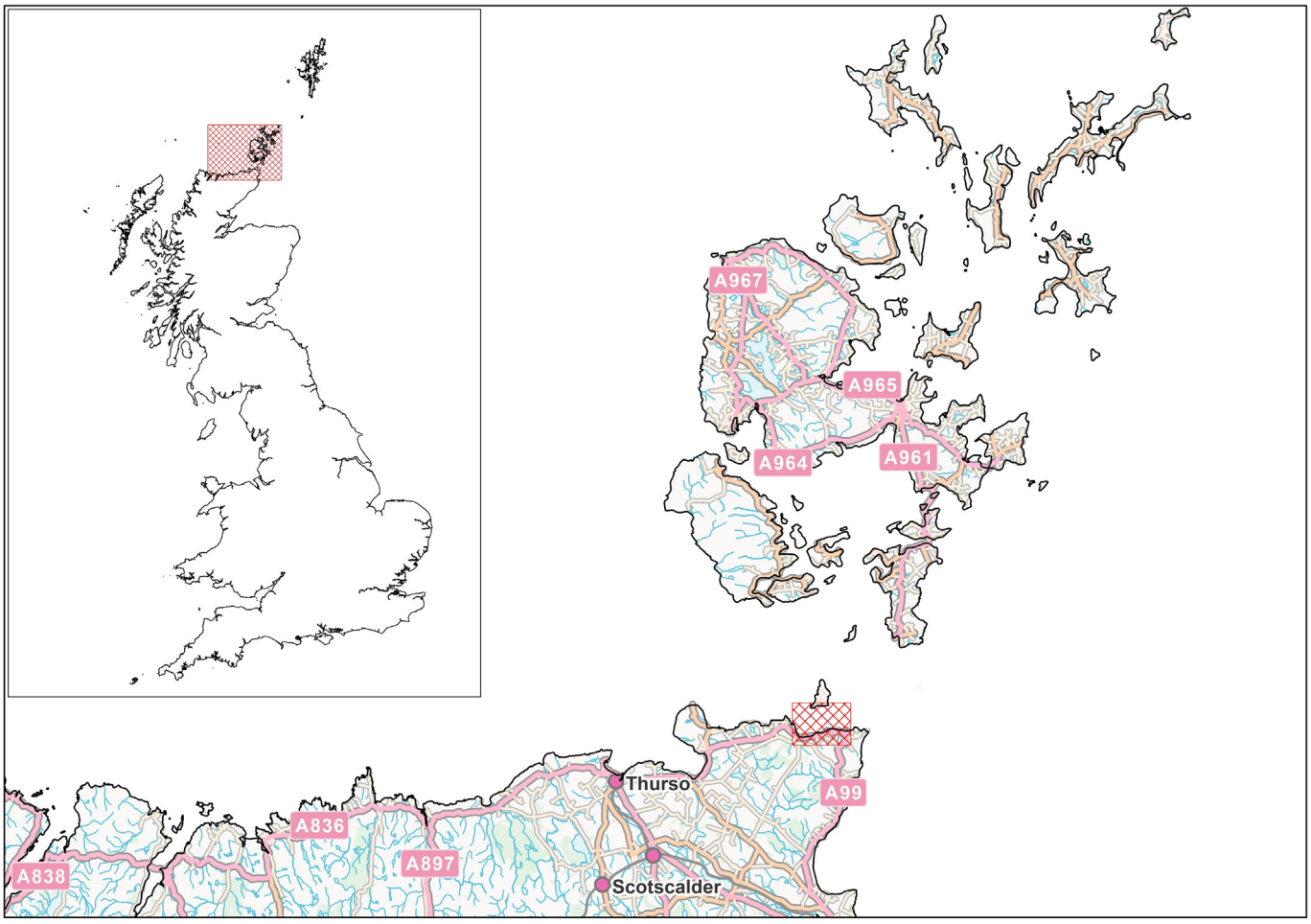

Fig. 1. (Inset) a map of the UK with the Pentland Firth and Orkney Waters marked with red hatching; (main) a map of the Orkney Islands and northern Scotland. The Pentland Firth is the channel between mainland Scotland and the Orkney Islands. The inner sound is marked by the red hatched area.

processes: firstly, additional currents can be induced via gradients in wave radiation stress and secondly the presence of waves increases turbulence at the bed, effectively increasing the friction felt by the current field. Inclusion of WCI in tidal resource estimation studies can lead to alteration in the predicted available resource [28,29]. Previous work looking at tidal range schemes has shown that changes to currents forced by energy extraction can alter tidal modulation of wave heights [30].

The impact of TSTs on sandbank morphodynamics been considered by various authors [16,31–39]. This work has shown that energy extraction at various locations can disrupt residual current gyres. Research has focussed on sediment transport by tidal currents alone with little consideration given to the relevance of including wave effects in the simulation. Purely simulating tide-driven processes may ignore key physical processes, Robins et al. [37], assessed the contribution of waves to bed sheer stress and concluded that wave-driven processes may be important. Fairley and Karunarathna [40] demonstrate, for the same sandbank as tested here, that wave action can magnify the impact of TSTs on bed level changes by considering short term simulations of characteristic storm processes. A 24 h period is simulated for storms from opposing directions (east and west) and tide only conditions, with and without turbines. The same model set up as presented here is used. Residual current magnitudes are altered by up to 10% when waves are included. Patterns of impact to bed level change are similar with and without wave action and are dictated by the presence of sand waves. The short time period and constant wave action used in that study means that more detailed simulations are required to better assess the importance of wave action for TST environmental impact studies.

Here, the analysis of Fairley and Karunarathna [40] is extended to consider morphodynamics over a spring-neap cycle with summer and winter wave conditions. Both baseline and extraction scenarios are considered. The aim of this paper is to both provide realistic simulations of morphological changes in the region and to assess if inclusion of wave processes makes a material difference to prediction of impacts.

2. Capabilities of MIKE3 regarding wave-current interaction

The MIKE3 2012 release was used in this analysis. Two key factors are involved with the alteration of currents by waves. Firstly wave radiation stress can induce a current. The hydrodynamic module takes radiation stresses (S_{xx}, S_{yy}, S_{xy}) from the wave module every time step. A uniform variation in radiation stress with depth is used for the vertical variation. Secondly, waves can increase the apparent bed roughness felt by a current. This is caused by increased turbulence intensity and shear stresses in the boundary layer forced by oscillatory wave motion (e.g. Ref. [41]).

The impact of tidal conditions on waves can be split between the variation in water depth and the presence of currents. Variation in

water depth is included in the simulations but is unlikely to be significantly altered by the level of energy extraction studied. Currents affect waves in a range of ways. The MIKE3 spectral wave model solves for the conservation of wave action N. In Cartesian co-ordinates this can be written:

$$\frac{\partial N}{\partial t} + \nabla \cdot (\vec{v} N) = \frac{S}{N} \tag{1}$$

where $N(\vec{x}, \sigma, \theta, t)$ is the wave action density, $\vec{x} = (x,y)$ is the Cartesian co-ordinates, t is the time, $\vec{v} = (C_x, C_y, C_\sigma, C_\theta)$ is the propagation velocity of the wave group in four dimensional space and S is the source term described below. $C_x, C_y, C_\sigma, C_\theta$ all depend upon $\vec{U}$, the current velocity vector and therefore may be affected by changes to the current field caused by energy extraction:

$$(C_x, C_y) = \frac{d\vec{x}}{dt} = \vec{c}_g + \vec{U} \tag{2}$$

$$C_\sigma = \frac{d\sigma}{dt} = \frac{\partial \sigma}{\partial d}\left[\frac{\partial d}{\partial t} + \vec{U} \cdot \nabla_{\vec{x}} d\right] - c_g \vec{k} \cdot \frac{\partial \vec{U}}{\partial s} \tag{3}$$

$$c_\theta = \frac{d\theta}{dt} = -\frac{1}{k}\left[\frac{\partial \sigma}{\partial d}\frac{\partial d}{\partial m} + \vec{k} \cdot \frac{\partial \vec{U}}{\partial m}\right] \tag{4}$$

where s is the space co-ordinate in the wave direction, m is the space co-ordinate perpendicular to the wave direction and d is the water depth.

The source term S can be written:

$$S = S_{in} + S_{nl} + S_{ds} + S_{bot} + S_{surf} \tag{5}$$

where S_{in} is the generation of wave energy due to wind (not considered in this study), S_{nl} is the transfer of energy through non-linear wave-wave interactions, S_{ds} is the dissipation of wave energy due to whitecapping, S_{bot} is the dissipation of wave energy due to bottom friction and S_{surf} is the dissipation due to depth induced breaking.

3. Study site

This research focuses on the Inner Sound of the Pentland Firth (Figs. 1 and 2). It is the narrow channel between the north coast of the Scottish mainland and the Orkney Islands which links the North Atlantic and the North Sea. The Pentland Firth is considered one of the world's most attractive sites for tidal energy extraction [42–47]. The Inner Sound is the sub-channel in the south of the

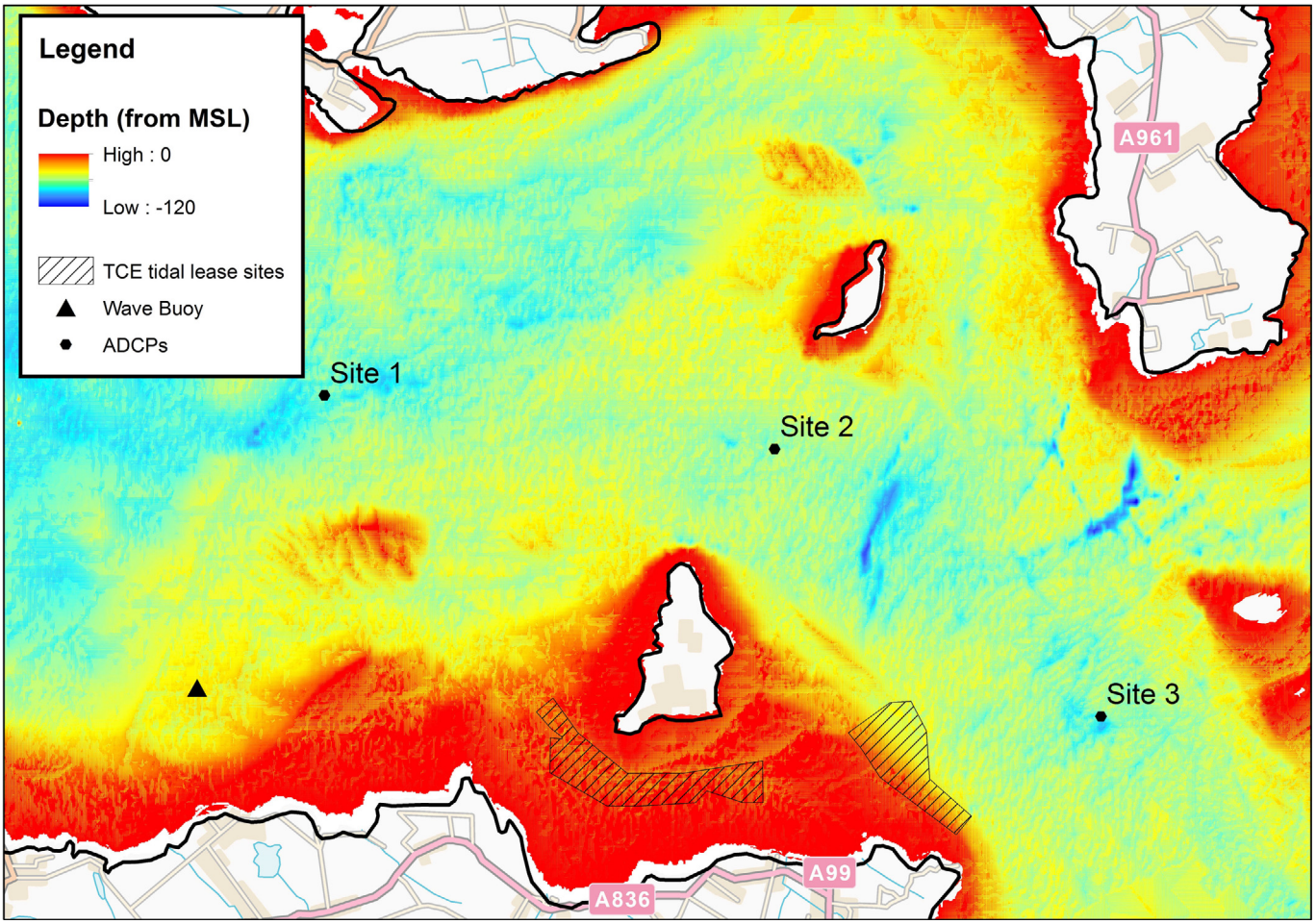

Fig. 2. A map showing a close up of the Pentland Firth and Inner Sound with the location of the three ADCPs and the wave buoy used for validation purposes marked. The locations of the two leased areas considered are shown as the hatched areas.

Pentland Firth, formed by the presence of the island of Stroma. The tidal regime in the region is dominated by the M2 component [34]. Phase differences of 2 h between the North Atlantic and North Sea [47] cause a hydraulic gradient which drives currents in the Pentland Firth in excess of 5 ms^{-1} at spring tide. Water depths in the main channel approach depths of 100 m below MSL, in the Inner Sound depths are less than 35 m below MSL. Interpretation of vessel mounted ADCP surveys has shown that in the Inner Sound there is tidal asymmetry in the region of maximum current between flood and ebb tides and that currents are not bidirectional [48].

Wave conditions in the region are some of the most energetic in Europe, however, sheltering and current effects mean that average wave heights in the Pentland Firth are 2 m [49], and that this reduces to the East and in the Inner Sound [50]. Winter conditions can be characterised by large, long period waves approaching from the SW – NW, whereas summer wave conditions are typically shorter period and approach from a more northerly direction [51].

Large areas of the Pentland Firth are swept bedrock due to the energetic waves and tidal currents in the region. The Pentland Firth has been identified as a bedload parting zone [52]. In regions of lower flow, sedimentary deposits exist including veneers of sand/gravel and fields of sand waves. These are often ephemeral features, only observable in some surveys [53]. Of greater interest when assessing TST impacts are the permanent sandbanks associated with headlands and islands. The largest of these sandbanks is the Sandy Riddle but this is sufficiently far removed from planned array locations that impacts at this early stage of development is unlikely [32]. In this study a sand bank to the east of the Island of Stroma (Fig. 2) is considered. This is comprised of coarse sand and gravel. Values for median grain size from grab samples taken at three locations from west to east along the sand bank centre line are 4.7 mm, 2.7 mm, 3.2 mm [2].

Recently more detailed surveys have been conducted of the sedimentology of the Inner Sound [54]. This study used grab samples and multi-frequency side-scan to map the seabed of the inner sound. Two sandbanks are identified: the large sandbank considered in this modelling study and a smaller oval sandbank, closer to the island of Stroma. Surveys of the large sandbank showed sand waves are present with wavelengths between 10 and 30 m on the northern flank, 10–15 m on the southern flank and smaller features over the crest with wavelengths around 5 m. Two surveys were conducted and while no difference in plan-shape or location of the bank was identified, a change in orientation of the dunes was noted [54]. They note that much of the retrieved sediment was platelet shaped shell fragments which makes the sand bank more resistant to erosion.

4. Methodology

The hydrodynamic (HD), spectral wave (SW) and sand transport (ST) modules of the DHI MIKE3 [55] suite were used in this analysis. These modules are fully coupled: that is, at every time-step currents and water depths for the SW module are read from the HD module; radiation stresses from the SW module fed to the HD module; and wave and current forcing from both the HD and SW modules is used by the ST module to compute sediment transport

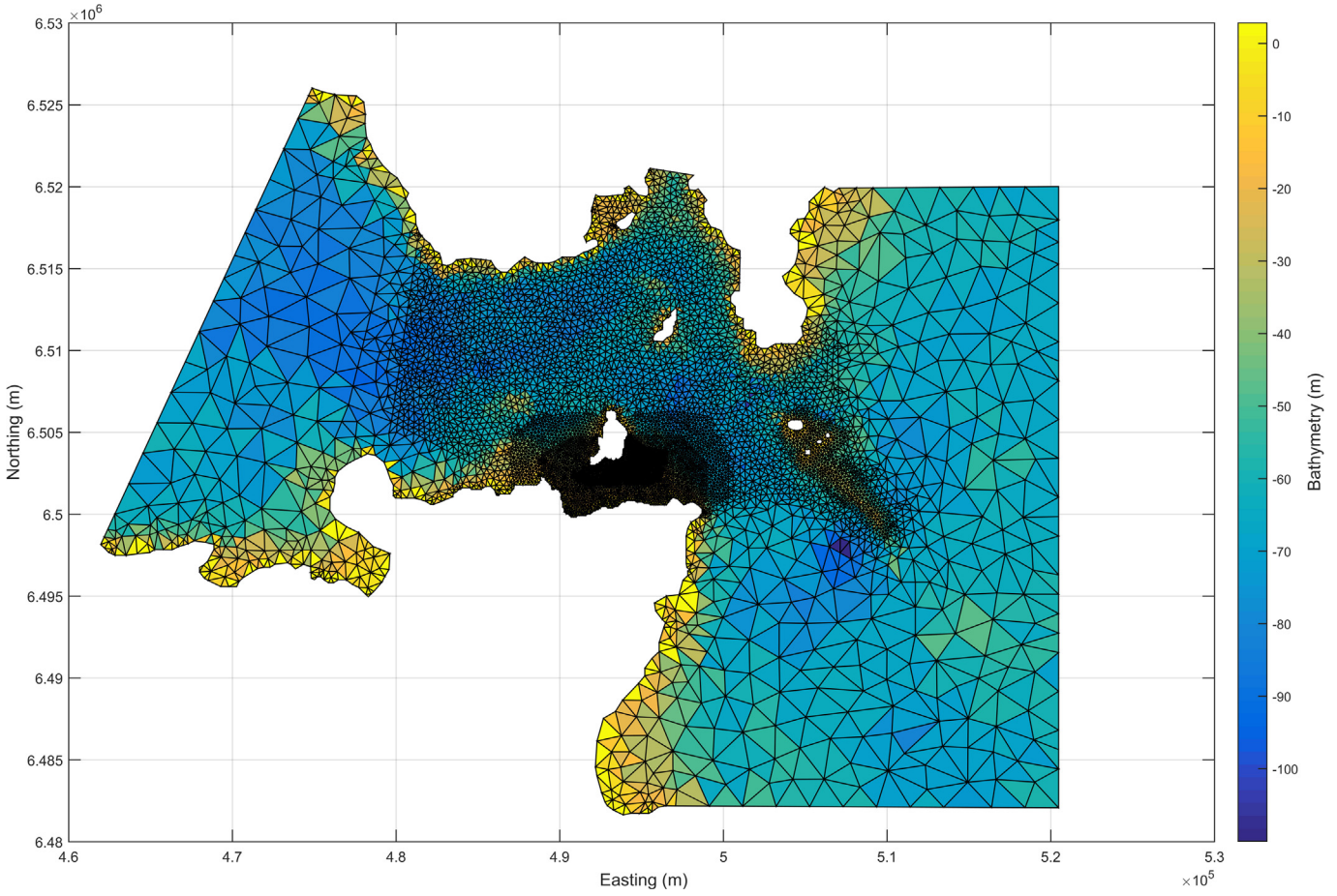

Fig. 3. The model domain and mesh used in this study.

and bed level changes. Morphological updating is also activated for all three modules every time step. Inclusion of wave current interaction in MIKE2012 is considered in Section 2.

4.1. Model mesh

The model mesh used is shown in Fig. 3, and a subset of the mesh around the sandbank in Fig. 4. An unstructured triangular mesh is used in this study which was developed using the DHI MIKE meshing tool and then refined using a MATLAB toolbox from DHI. Element areas ranged from 2,000,000 m^2 in the outer regions to less than 500 m^2 over the sandbank. The size of the domain is constrained by computational restrictions of running a coupled HD-SW-ST model, however previous work has shown that the mesh is sufficiently large for analysis of tidal steam energy impacts on regional sediment transport [32].

4.2. Sediment data

Spatially varying sediment size (Fig. 5) and layer thickness is included over the model domain. A variety of sources are used for the sediment data: data contained within environmental statements, British Geological Society grab samples [56] and Marine Scotland Science benthic video trawls. Natural neighbour interpolation was used to interpolate spatially between sample points to a regular grid which could be applied to the model domain. Areas of mobile sediment and swept bedrock were defined manually using textural surfaces derived from de-trended multibeam data. Fuller description of the approach to sediment in this analysis can be found in Fairley et al. [32]. Initial layer thickness was set to 5 mm for all areas of swept bedrock in the domain and to 5 m for areas defined as areas of mobile sediment. Within the model, a threshold sediment thickness was also set to 5 mm which reduces transport rates for layer thicknesses below this value. This reduction follows a parabolic formula [55]:

$$Q_{t,\,reduced} = Q_t(\Delta h/\Delta h_{crit})^2 \tag{6}$$

Thus, the 5 mm veneer over the bedrock can be considered to represent the sediment that is present within crevices in the bed rock and within interstitial spaces between cobbles and boulders. The parabolic formulation is included since sediment in these spaces will be less easily transported than exposed sediment.

4.3. Inclusion of turbines in MIKE3

The two tested arrays were implemented as series of individual turbines. MIKE3 has an inbuilt turbine tool that allows inclusion of turbines as sub-grid structures by specification of turbine location, hub height, turbine diameter and lift and drag curve. Actuator disk theory is then used to determine a momentum sink. This momentum sink is spread evenly between all vertical layers occupied by the turbine swept area. The velocity used is the average of the cell velocity of the cells occupied by the turbine for all vertical layers occupied by the turbine.

The turbine properties were taken from work within the UK EPSRC funded Terawatt project that defined a generic turbine design for academic work on hydrodynamic impact via discussion with developers [57]. This hypothetical turbine had a rated power of 1 MW and a turbine diameter of 20 m. In this study the turbine hub height was specified as 17 m above the sea bed. The cut in

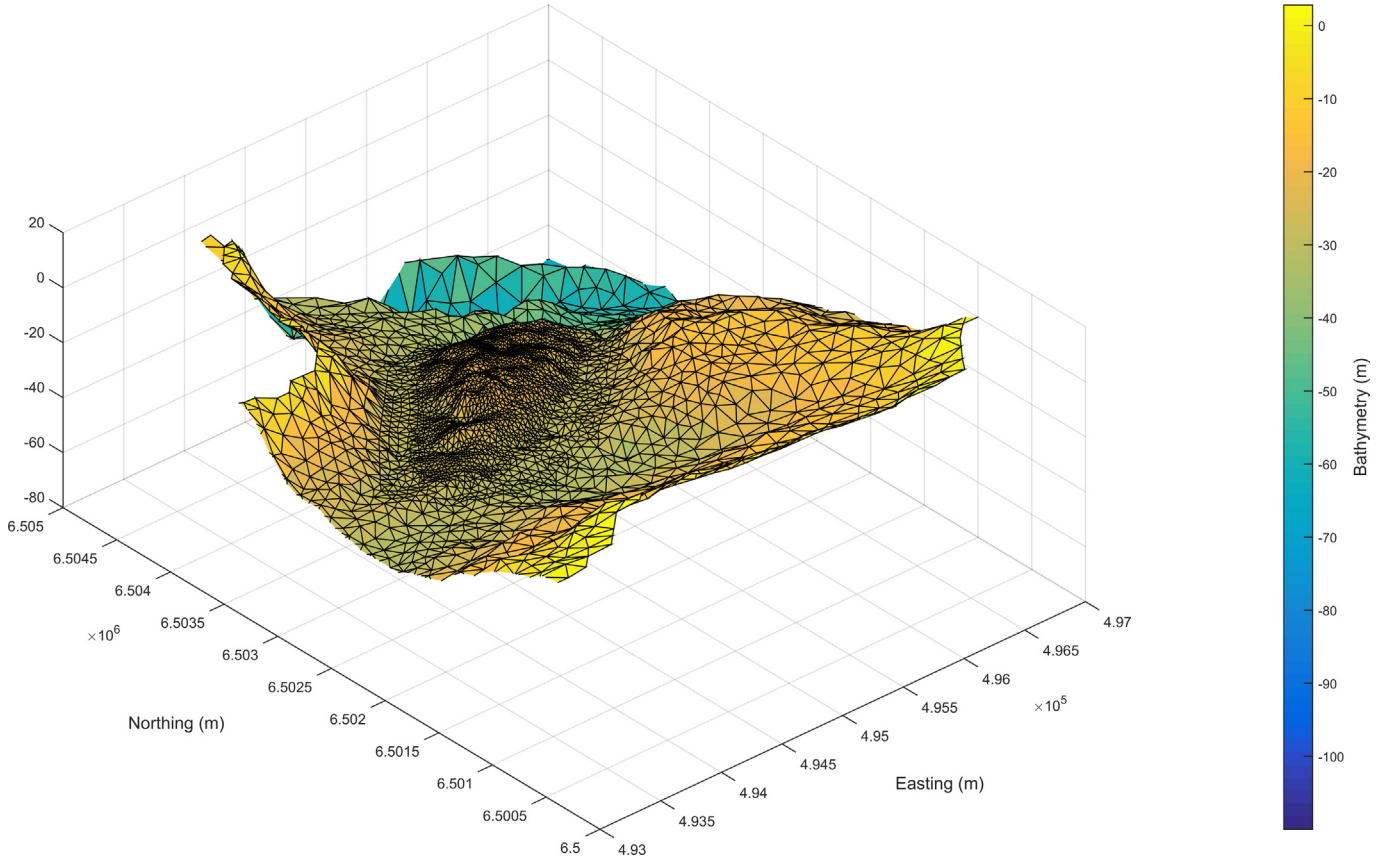

Fig. 4. A subset of the mesh over the studied sandbank showing the increase in mesh density and the shape of the sandbank. Note the large sand waves present.

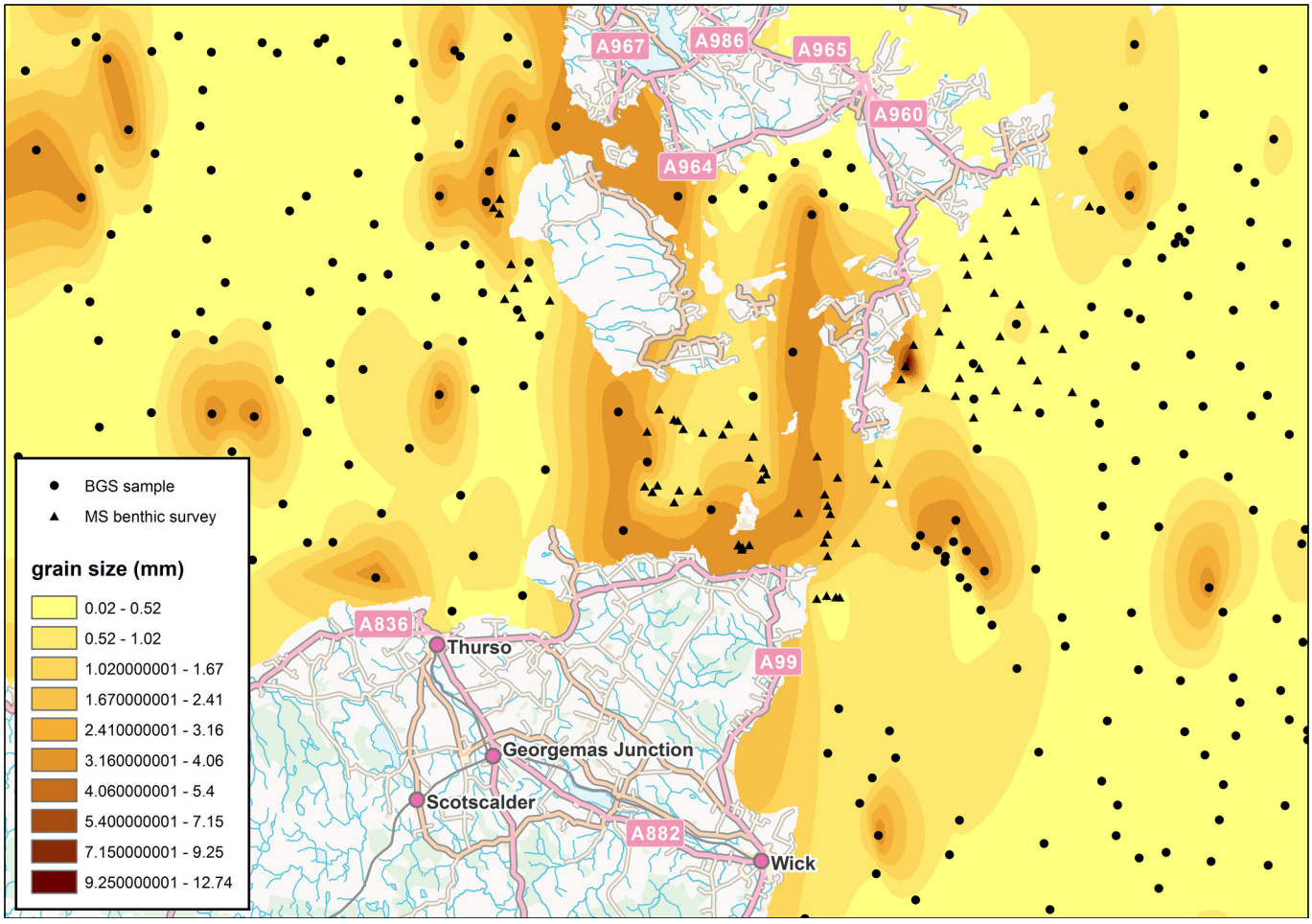

Fig. 5. Variation in median sediment size based on BGS sediment samples and MSS benthic surveys (reproduced from [40]).

speed was set to 1 ms^{-1} and the cut-out speed to 4 ms^{-1}. A plot of the thrust co-efficient (C_T) against speed for the hypothetical turbine is shown in Fig. 6. Array layouts were determined by Marine Scotland Science [58]. Turbines were spaced by 160 m in the direction of flow and 50 m laterally. 400 turbines were included in the Inner Sound site and 100 turbines in the Ness of Duncansby site. The array layouts for the two considered leased areas are shown in Fig. 7. .

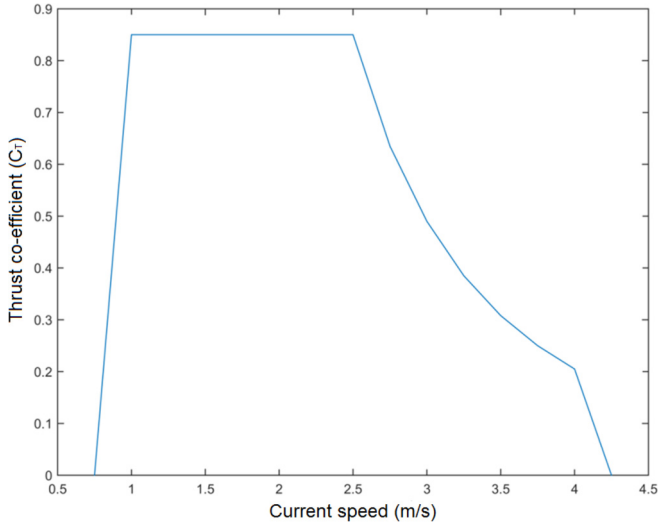

Fig. 6. A plot of the hypothetical thrust co-efficient curve developed within the Terawatt project and used in this study.

4.4. Test scenarios and boundary conditions

Two time periods are considered: a winter spring neap cycle and a summer spring neap cycle. For both time periods, the model is run for scenarios with and without turbines and with and without the wave module being activated. Therefore, in total, 8 simulations were run: summer, tide only, no turbines; summer, tide only,

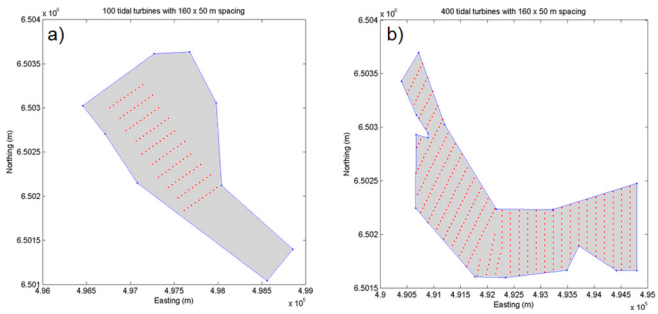

Fig. 7. A plot of array layouts as determined by Marine Scotland Science and used in this study: a) the Ness of Duncansby site; b) the Inner Sound site.

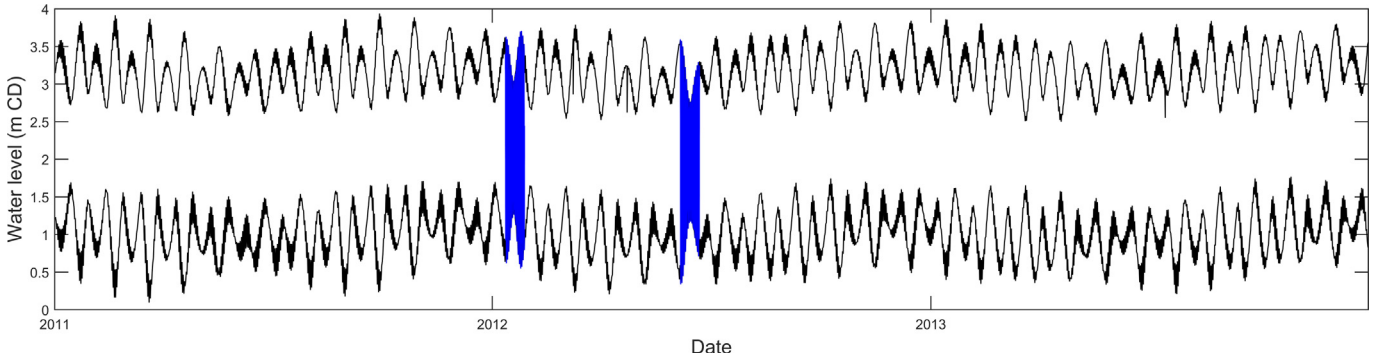

Fig. 8. The tidal envelope at Wick (black lines) and the winter and summer scenario tide periods (blue shading).

turbines; summer, waves included, no turbines; summer, waves included, turbines; winter, tide only, no turbines; winter, tide only, turbines; winter, waves included, no turbines; winter, waves included, turbines.

Summer and winter scenarios were taken from 2012 for comparison of bed level changes under different conditions. A winter scenario from 12/01/2012–27/01/2012 and a summer scenario from 06/06/2012–21/06/2012 were chosen. These periods were chosen due to co-incidence of availability of input boundary conditions and availability of wave data from a wave buoy deployed by UHI in the Pentland Firth.

The astronomical tidal envelope for the nearest National Tidal and Sea Level Facility gauge at Wick is shown in Fig. 8 for 2011–2013 [59] and water levels for the two tested time periods. The Wick Gauge is located further south than the study area, outside the bounds of the maps in Figs. 1 and 2, at 58° 26.458′ N, 3° 5.179′ W. Both time periods are representative of the tidal regime in general, neither containing particularly large spring tides nor small neap tides. The winter scenario has slightly greater tidal ranges than the summer and hence faster currents.

For the summer scenario, waves in the inner sound are largely incident from the east. They are lower period than the winter wave

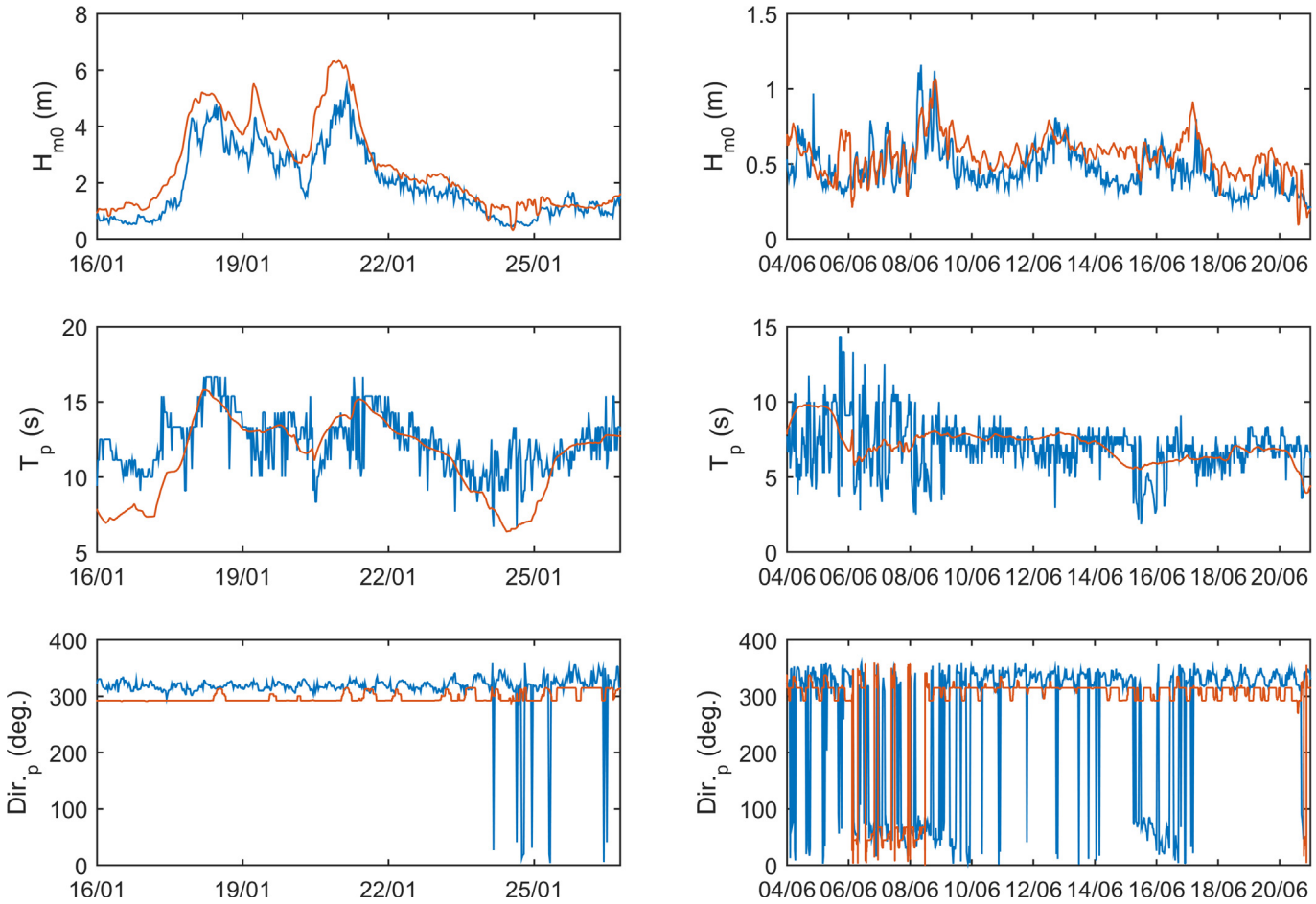

Fig. 9. Modelled (red) and measured (blue) wave parameters for the January (left hand column) and June (right hand column) test periods.

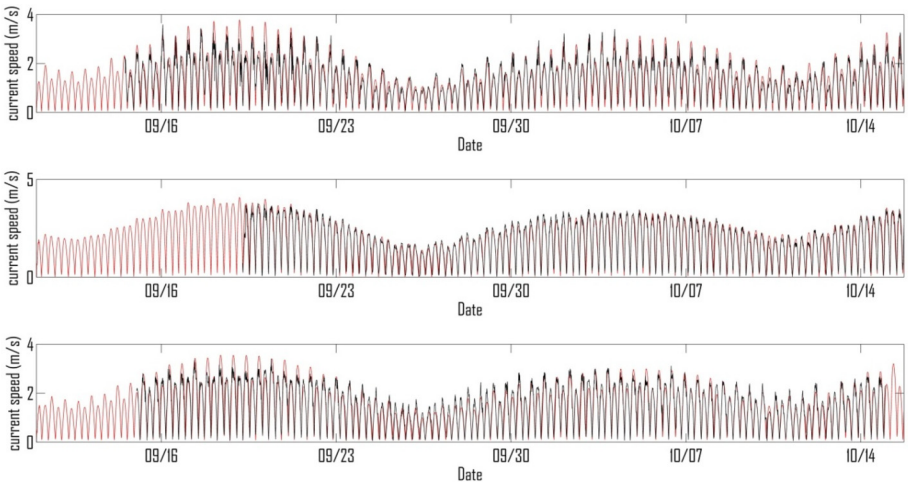

Fig. 10. A comparison between measured (black) and modelled (red) depth averaged current speeds for the three sites marked in Fig. 1. Site 1 is the upper panel, site 2 the middle panel and site 3 the lower panel.

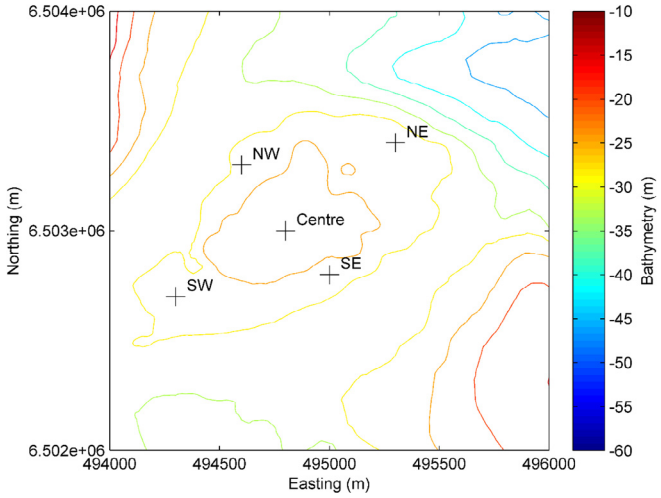

Fig. 11. A plot showing the sandbank and the location of five data extraction points.

conditions, although magnitudes of wave heights are similar. For the winter scenario, wave direction is more variable with waves over the sandbank incident from between the west and north for much of the more energetic times (See Figs. 11 and 12 in Section 5.1). Tidal boundaries were taken from the DHI global tidal atlas and elevations specified at all boundaries. The elevations varied along the boundaries based on the global tidal atlas data. A wave model created by ABPMer for the Pentland Firth and Orkney Waters using MIKE21 SW [49] was run to provide input wave conditions at all model boundary conditions.

4.5. Model validation

Model performance was evaluated by comparison with ADCP data in the centre of the Pentland Firth for current data and a wave buoy to the west of the Pentland Firth (locations in Fig. 2). No calibration was conducted for the wave model since only one comparison point was available. Instead it was assumed better to rely on the default values and accuracy of model physics rather than tune for a solitary point which may not be representative of the domain as a whole. Comparison between measured and modelled wave parameters was conducted for the two test periods of 12–27 January 2012 and 6–21 June 2012 (Fig. 9). Validation was conducted using the coupled wave and tidal model. Measured wave parameters were available on an hourly basis. The coefficient of determination (r^2) and root mean squared error *(RMSE)* values for the different parameters and test cases are listed in Table 1. Visually, the model well represents the shape of the wave height record. For the winter period there is a slight over prediction of wave height, especially during storm periods. This over prediction is less in the summer period as evidenced by the lower *RMSE*. For both summer and winter the higher frequency variability is not represented. For the winter wave direction there is a bias of 8°: the mean of the measured data during this period is 315° and the mean of the modelled data is 307°. A similar bias is shown in the summer wave direction plots.

Fig. 10 shows comparison of model results against ADCP data for the three sites marked on Fig. 2. The ADCP data consisted of time series of 10-min averaged velocity profiles which were depth averaged for the purpose of validation. The ADCP data spanned 30 days from 14/09/2001. Visually the comparison is good, root mean square errors were from 0.26 to 0.33 ms^{-1}, which is considered acceptable. A lag of approximately 7 min between modelled and measured data was observed. At sites one and three, the model over predicted current speeds. For these two sites peak flood and ebb currents are asymmetrical and maximum currents occur on opposing halves of the tidal cycle, caused by presence of a current jet between the two islands in the Pentland Firth This jet is present in the western half of the Pentland Firth on the ebb and on the eastern half on the flood. Undocumented communication suggests that there may be errors in the ADCP measurements at times of peak current caused by unwanted movement of the sub-surface float to which the ADCP was attached. Therefore, it is difficult to determine whether the discrepancy is entirely down to poor model performance.

No sediment transport or bed level data was available to calibrate the sediment transport module for this study. However, confidence can be gained by the good validation of waves and currents which means direction of transport is likely to be correct. Additionally, the model equations and architecture have been validated against analytical solutions within the model documentation [60] and against measured sediment transport for combined waves and currents [61]. Various authors have demonstrated the ability of the MIKE suite of models to replicate sediment transport in real world conditions with good results (e.g. Refs. [62–64]).

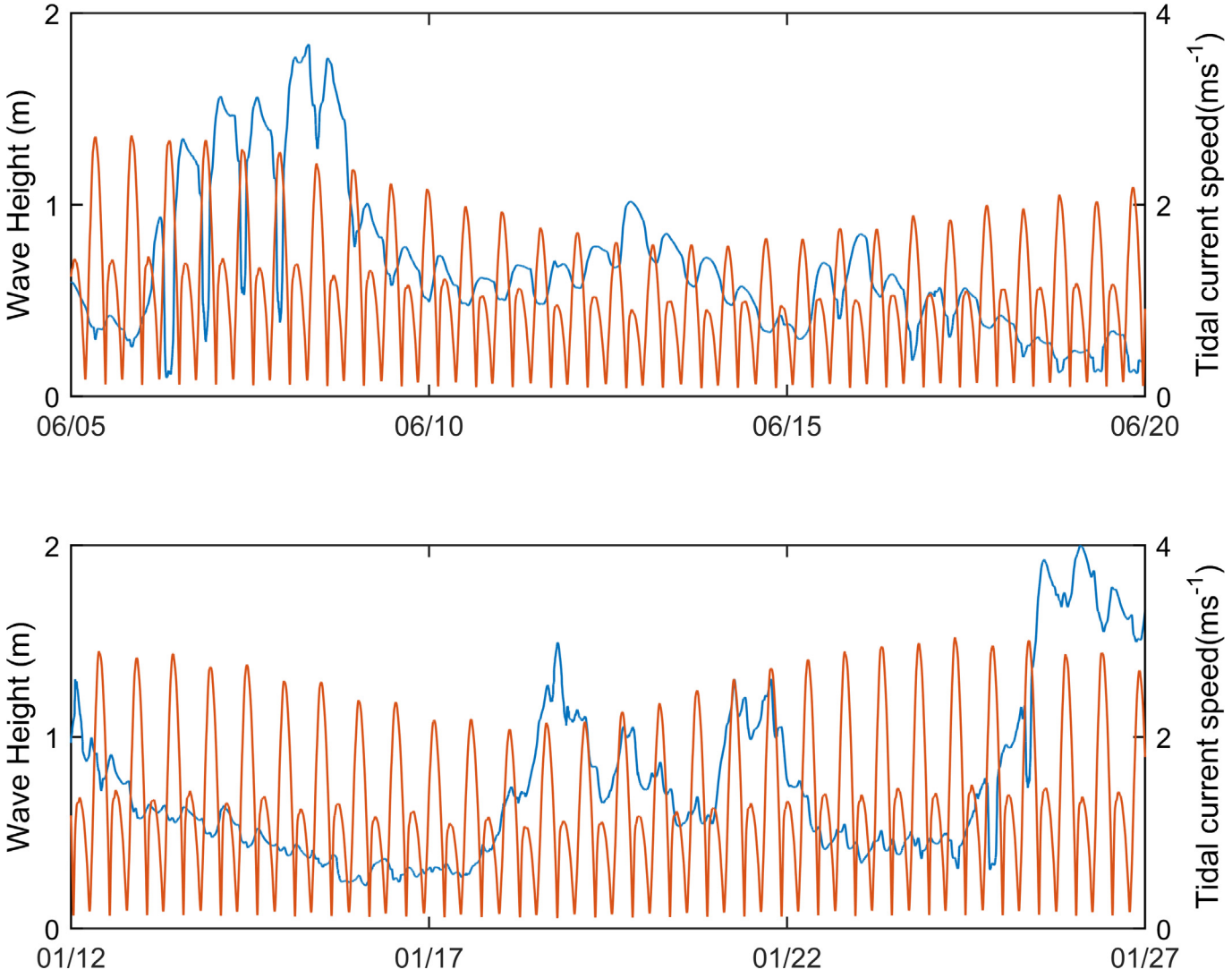

Fig. 12. Wave heights (blue) and tidal current speed (orange) for summer (upper panel) and winter (lower panel) extracted at the point over the centre of the sand-bank.

Table 1
RMSE and r^2 for wave parameters.

	Hm0 (m)		Tp (s)		Dir.p (deg.)	
	Winter	Summer	Winter	Summer	Winter	Summer
RMSE	0.8	0.15	2.1	1.7	41	119
r^2	0.3	0.865	0.45	0.05	0	0.12

5. Results

In this section results from the numerical modelling are presented. The parameters considered are: wave height and direction; depth averaged current velocities; total load magnitude; vertical bed level change; and total sandbank volume change. Focus is primarily given to five points over the sandbank of interest. Parameters are plotted as time series where the parameters are averaged every 10 min. Values at the tested points were calculated via interpolation from surrounding nodes which was conducted automatically within the MIKE software. The five points are shown in Fig. 11. One point is a central point on the crest of the sandbank, one on each lateral flank (NW and SE) and one on each longitudinal flank (SW and NE). Particular attention is given to the point on the crest. Due to the irregular morphology of the sandbank, sensitivity of the results to point location over the crest was assessed and found to not dramatically impact results.

5.1. Wave conditions

Predicted wave heights in the inner sound show substantial tidal modulation, especially for the summer case. Fig. 12 shows predicted wave heights in the Inner Sound for both summer and winter scenarios overlaid on the tidal current speeds. Data is taken from the point on the crest of the sandbank. Drops in wave height are coincident with maximum tidal currents. This pattern is much less noticeable for the winter case. The difference is due to the wave direction (Fig. 13). Modelled wave direction in the inner sound for the summer case is consistently from the east which is aligned with and opposed to flow direction of peak flood current speed. Wave direction in the winter case is more variable, being from the north west for much of the time and from the east at the start and end of the time period. A tidal modulation of direction is also observable for both scenarios. Despite the obvious tidal influence on wave

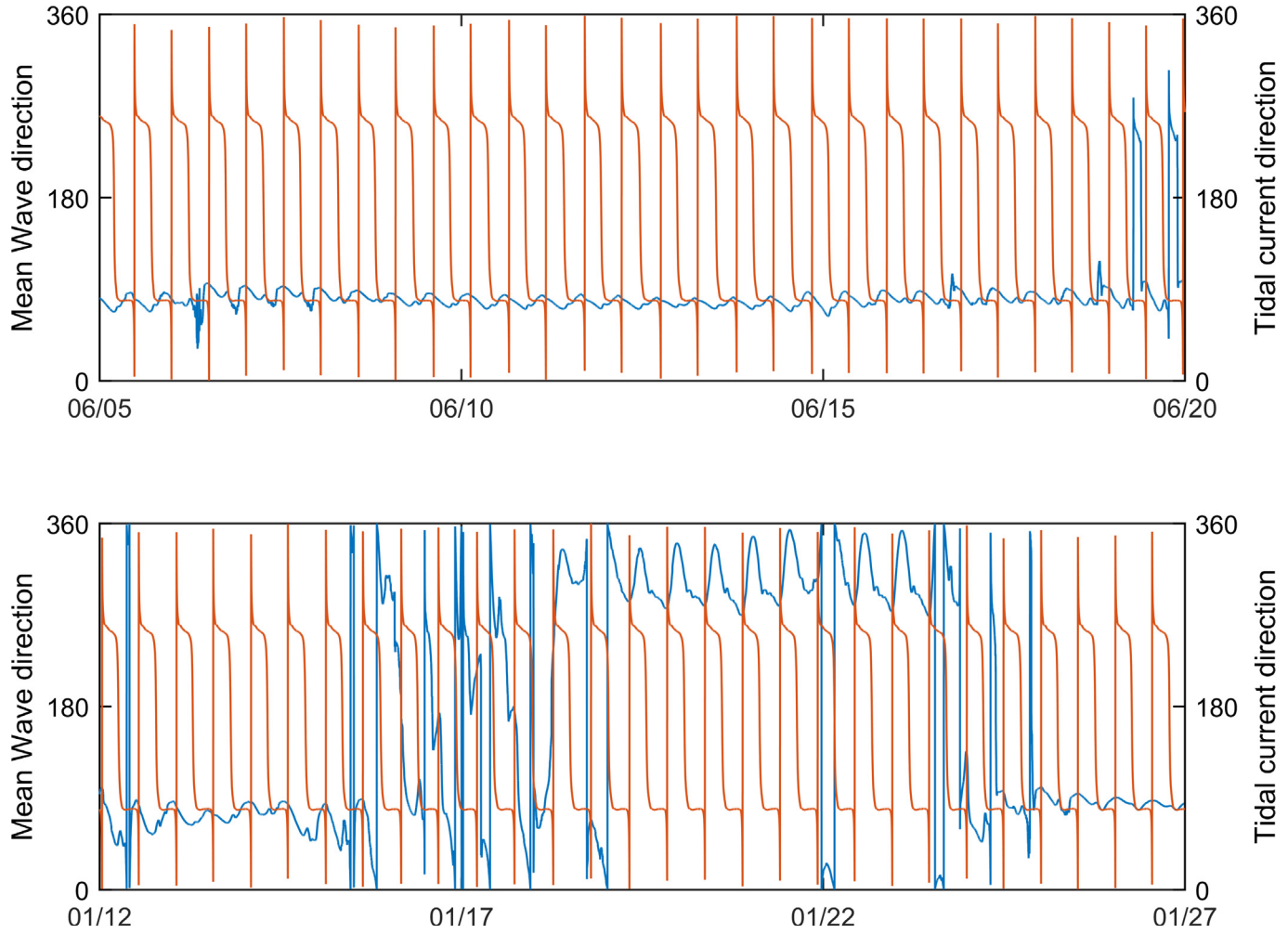

Fig. 13. Mean wave direction (blue) and tidal current direction (orange) for the summer scenario (upper panel) and the winter scenario (lower panel). Note that directional conventions are opposite for waves and current: wave direction is the direction the wave comes from and current direction the direction the current goes to.

conditions, deployment of turbines does not alter currents sufficiently to impact on wave conditions over the sandbank: differences in model prediction of significant wave height are typically less than 2 cm and at most 5 cm when tidal turbine energy extraction is included.

5.2. Hydrodynamics

Inclusion of the wave module can alter simulated hydrodynamics over the tested sandbank, although noticeable changes only occur under certain storm conditions. Fig. 14 shows plots of depth averaged u and v velocities for the point on the crest of the tested sandbank for both scenarios time periods and the difference caused by inclusion of waves. For the summer case it can be seen that there is minimal difference in depth averaged velocities throughout the record with differences typically much less than 0.01 ms^{-1}. For the winter case, one storm event shows differences in depth averaged velocities of over 0.1 ms^{-1}. This event occurs when waves are incident from the north-west, events from the east do not cause the same difference. The points extracted on the sandbank flanks showed similar results (not shown).

The primary objective of this paper is to ascertain whether inclusion of waves in simulations affect the impact of TSTs on morphodynamics. To answer this, attention is given to the 6 day subsection of the winter scenario where inclusion of waves are shown to alter u,v velocities to the greatest extent. Fig. 15 shows both the change in u,v, velocities caused by energy extraction and the difference in that change when waves action is included in the simulation. Points on the north-western flank, the crest, and the south-eastern flank are considered. For the north-western flank, the differences in velocity are primarily positive and correspondingly the change caused by wave action is also primarily positive. The point extracted on the south eastern flank shows the opposite trends whereas the point extracted on the crest is more symmetrical between positive and negative change. The change in impact is relatively small however, with change being within ±5% of the tide only impact for over 80% of the time. There is little clear shape to this difference in impact.

5.3. Sediment transport

Time series of the magnitude of total load (the sum of suspended load and bed load) sediment transport volumes and the impact of energy extraction show broadly similar patterns for all four scenarios although magnitude of total load varies. Therefore just the summer case with no waves is described here (Fig. 16).

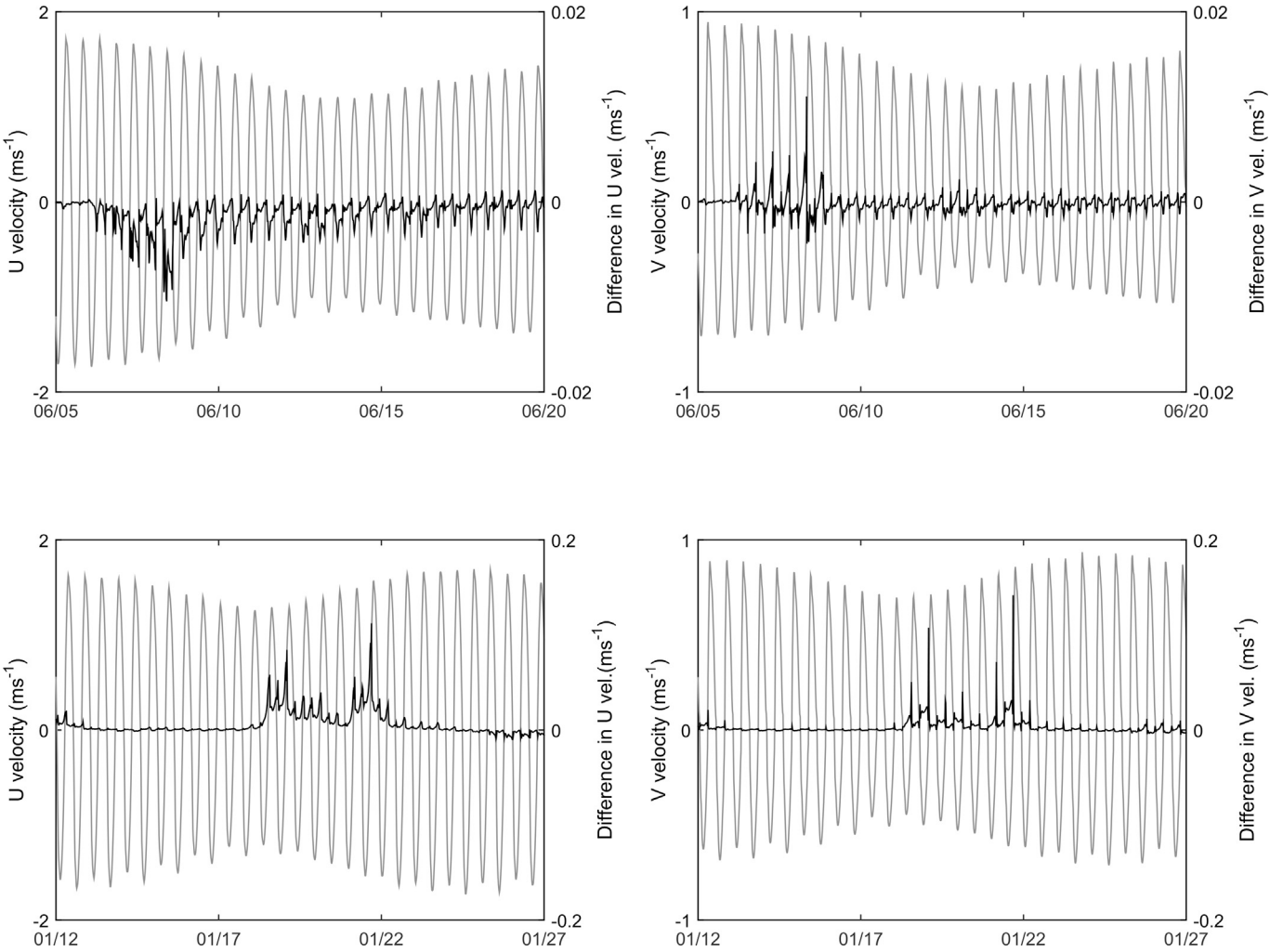

Fig. 14. Depth averaged u and v velocity components (grey, left axis) and difference in u and v velocities (black, right axis) caused by inclusion of wave action. The summer scenario is in the upper two panels and the winter scenario in the lower two panels. Note the change in scale.

There is an asymmetry in total load magnitude between flood and ebb tides. For the points on the centre, SE and SW, magnitude of total load is greater on the flood tide (flow from west – east). The opposite is true for the NW and NE points. Magnitude of total load is greatest for the point on the SE flank which is furthest into the main channel. Implementation of turbines reduces the magnitude to total load transport. There is still an asymmetry in the total load transport, however for all 5 points the magnitude of total load transport is greatest on the flood tide. This change represents the removal of the residual gyres as described in previous work [33,40]. The relative magnitude of the total load between points is altered with greatest magnitude of transport observed on the SW point of the case with turbines. The shape of change caused by turbines is not uniform between points. For the central point for the first part of the flood tide there is a reduction in magnitude, with an increase in magnitude for the second part.

Inclusion of wave action increases the magnitude of sediment transport. This is the case for all tested cases at all five points over the sandbank. Fig. 17 shows time series of the difference between tide plus wave and tide only driven transport for both summer and winter with and without turbines. The differences are asymmetric with greater differences for the flood tide when currents are directed towards the east for all five points. The magnitude of difference is significantly larger than the magnitude of the tide only total load transport (4–5 times greater on average).

Similar patterns are shown for the difference in turbine impact on total load sediment transport caused by waves. Fig. 18 shows the wave induced difference in turbine impact on sediment transport, where:

$$\textit{Wave induced difference in turbine impact on sediment transport} = (TLM_{TW} - TLM_{NoTW}) - (TLM_{TT} - TLM_{NoTT}) \quad (7)$$

where TLM is the total load magnitude and the subscripts are: TW, turbines and waves implemented; NoTW, no turbines but waves implemented; TT, turbines implemented for the tide only case; NoTT, no turbines implanted for the tide only case. A subset of the results are shown, it can be seen that for the ebb tide differences in impact are similar for all points whereas for the flood tide there are greater differences in the shape of the difference in impact.

5.4. Morphological changes

Morphological changes are variable in both direction and magnitude over the tested sandbank. It is believed this variation

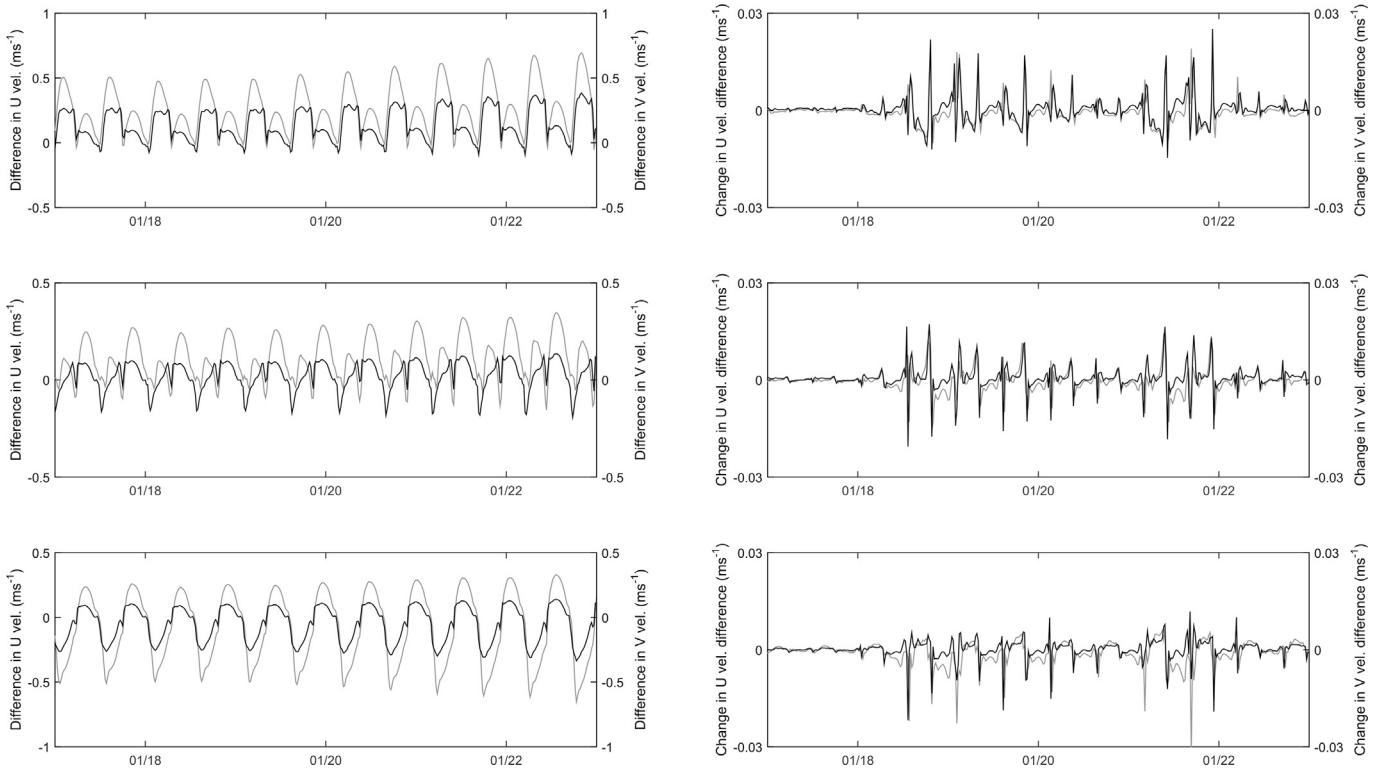

Fig. 15. Plots of difference in u (grey) and v (black) velocity components caused by turbine implementation for the tide only case for (a) the north west flank, (b) the central point and (c) the south eastern flank; change in that difference caused by inclusion of waves in the simulations for u (grey) and v (black) components for (d) the north west flank, (e) the central point and (f) the south eastern flank.

in direction is caused by the large sand waves present on the sandbank. Fig. 19 shows an example of this: changes to bed level over the winter test case with waves included is shown for both the natural and energy extraction cases. Only a close-up of the considered sandbank is shown in the figure. For the natural case change is focused on the southern flank of the sandbank whereas for the energy extraction case change is focused over the crest. Further examination of the spatial variation in bed level changes is presented in Fairley and Karunarathna [40]. Examination of time series of bed level change shows that similar responses are predicted for both the summer and winter scenarios. The three points on the longitudinal axis (SW, centre and NW) show similar patterns, while the points on the lateral flanks (SE and NW) show different behaviour. Therefore in Fig. 20 only the winter scenario is presented for the central, SE and NW points. For clarity of behaviour, bed level is plotted such that the bed level at $t = 0$ is set to 0 for all points. Certain patterns are consistent between all points and scenarios: the semidiurnal variability in bed level is greater for the scenarios including wave in their simulations. Rates of change are faster for start and end of the time series during spring tides and flatter in the middle during neap tide. Differences in bed level are greater for the points on the two flanks compared to the central flank. At the central point, the scenarios including waves show that despite differences with and without turbines over the tested time period the end result is very similar with an accretion approaching 0.03 m. For the tide only scenarios, erosion is shown and inclusion of turbines reduces this erosion. Different behaviour is shown on the NW flank point: for the no turbine case there is minimal change (tide only) or slight accretion (waves included) whilst when turbines are included erosion is shown with greater erosion when waves are included. On the south eastern flank, the no turbine cases both show accretion, with greater magnitude for the scenario with waves included. Implementation of turbines reduces the level of accretion; the reduction is a similar level for both tide-only and wave scenarios.

In order to provide information on bulk changes to the tested sandbank, Table 2 shows volumetric changes over the spring neap cycles for the whole sandbank. Not only are the calculated volume changes for the eight cases presented but differences in volume change between scenarios also given. Differences caused by turbine implementation are shown as are differences in volumetric change when waves are included in the simulation. The area of the sand bank encapsulated by the −25 m MSL was used in the volume calculations. For reference the total volume of the sandbank above the −25 m contour is ~658,000 m^3 and thus the largest volumetric change (the winter scenario with turbines and waves) is about 1.5% of the total volume for the tested 14 day period. For the tide only cases there is a reduction in volume over the two tested spring neap cycles. Inclusion of wave action reverses this and there is an increase in volume over the sandbank. There is a greater increase in volume for the winter case. For the tide only simulations turbines implementation reduces the amount of erosion, for the simulations with waves turbines cause an increase in accretion; thus in both cases there is a positive difference in volume change caused by turbines. The difference in volume change caused by inclusion of turbines ranges from 0.07% to 0.4% of the total volume. The predicted impact is greater for the case with waves. The difference between the tide only and wave cases are greater than the difference between the turbine and no turbine cases being between 1 and 1.8% of the total sandbank volume.

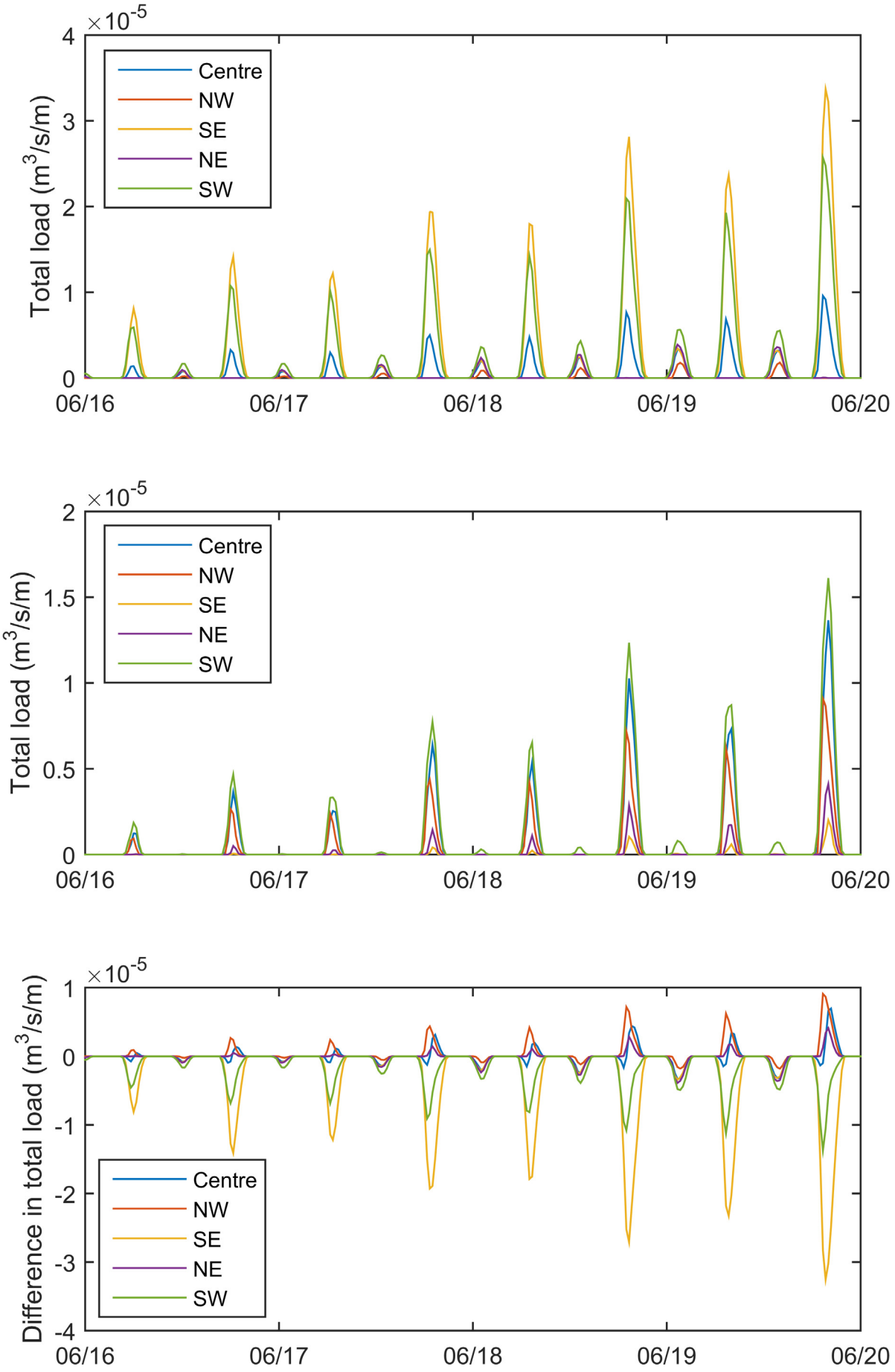

Fig. 16. Total load magnitudes for the no turbine case (upper panel), the turbine case (middle panel) and the difference between the two (bottom panel). All plots are for the June tide only case. The five lines described in the legend refer to the five points displayed in Fig. 11.

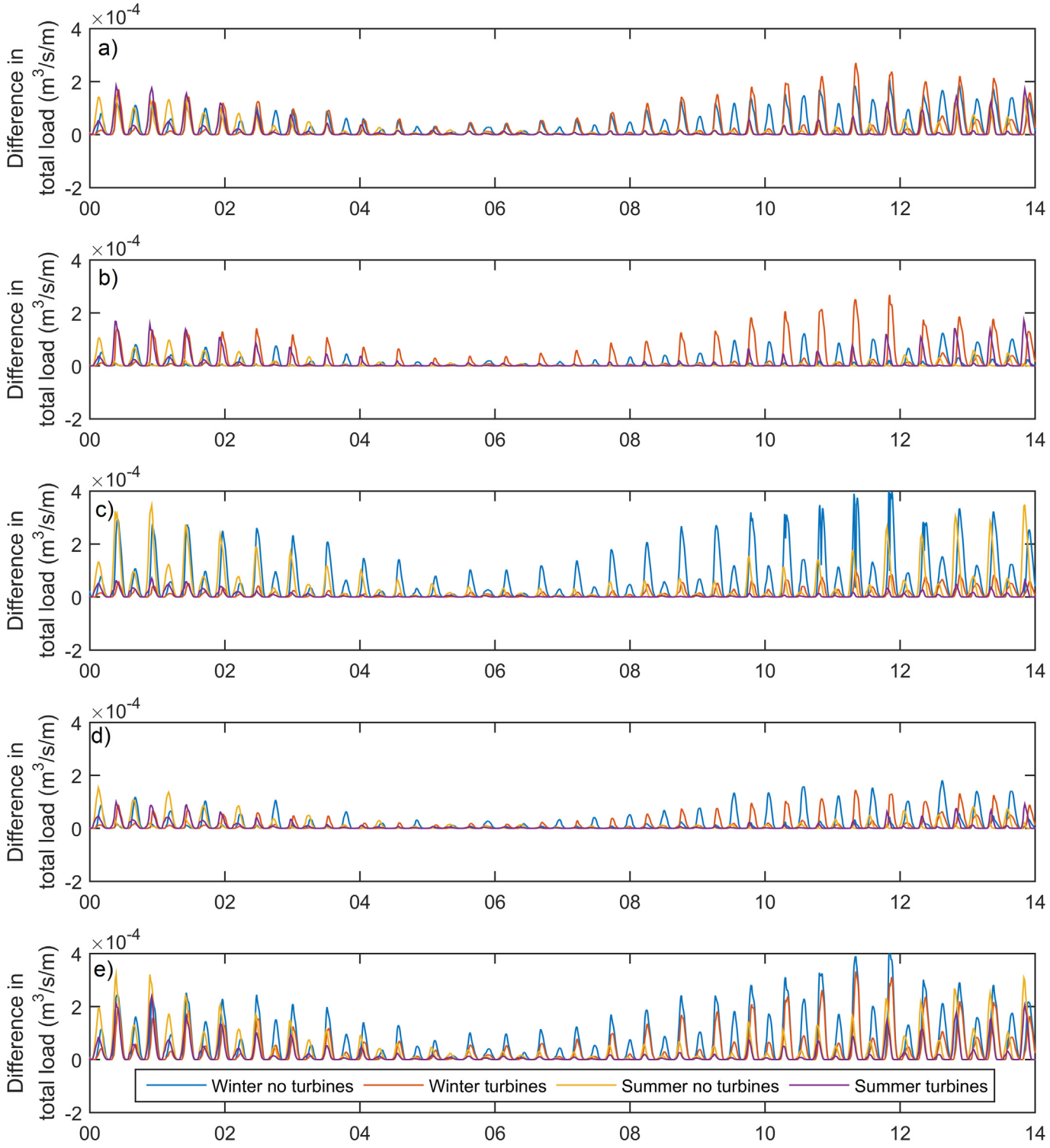

Fig. 17. The difference in total load caused by inclusion of waves in the simulations for the winter and summer cases with and without turbines (second panel); and the summer case without turbines (third panel) and with turbines (bottom panel). Results are shown for: a) the central point; b) the NW point; c) the SE point; d) the NE point and e) the SW point. The five locations described refer to the five points displayed in Fig. 11. Time is given as days from peak spring to enable comparison of summer and winter periods.

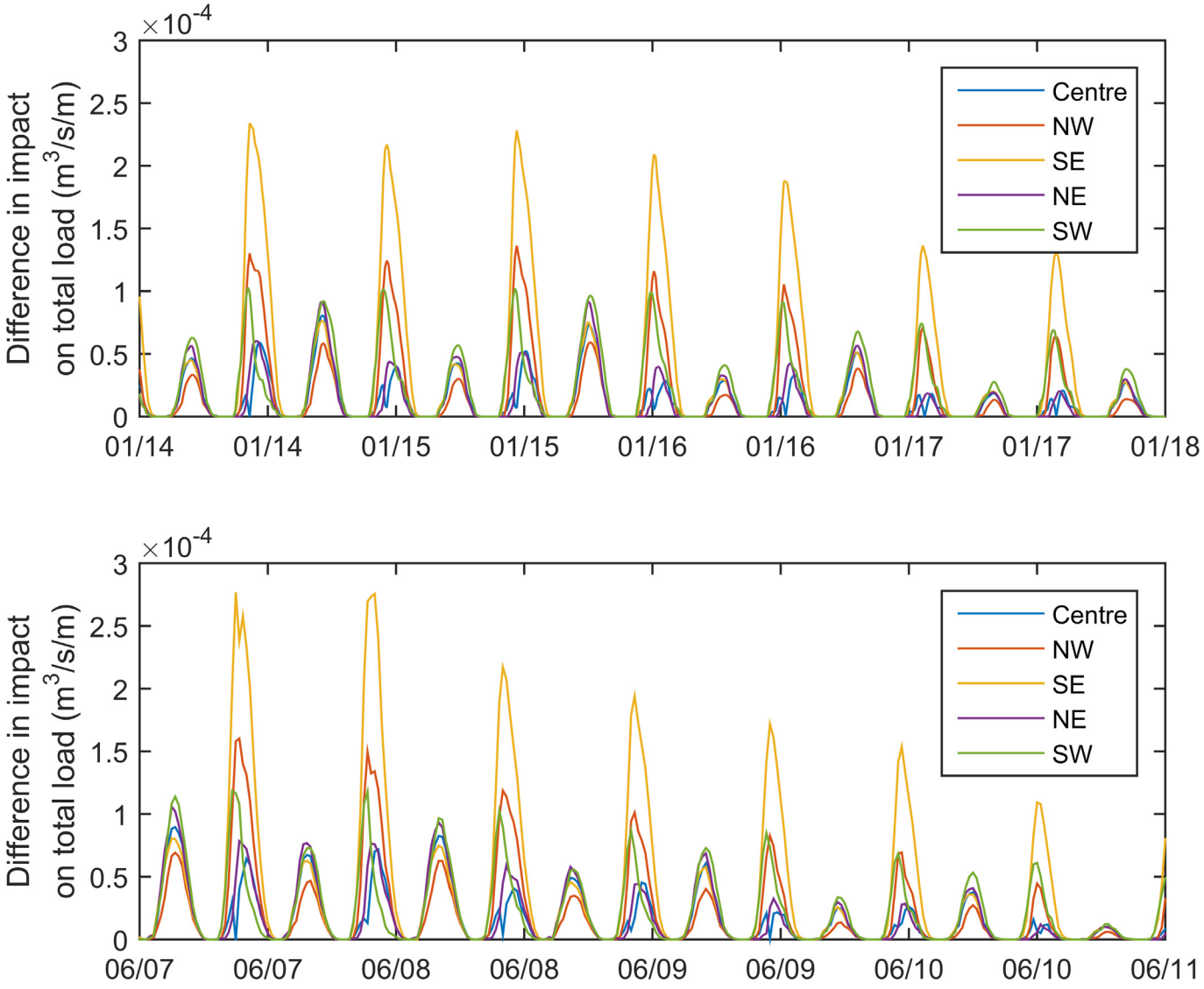

Fig. 18. The difference in impact of turbines on total load transport between the simulations with and without waves for the winter case (upper panel) and the summer case (lower panel).

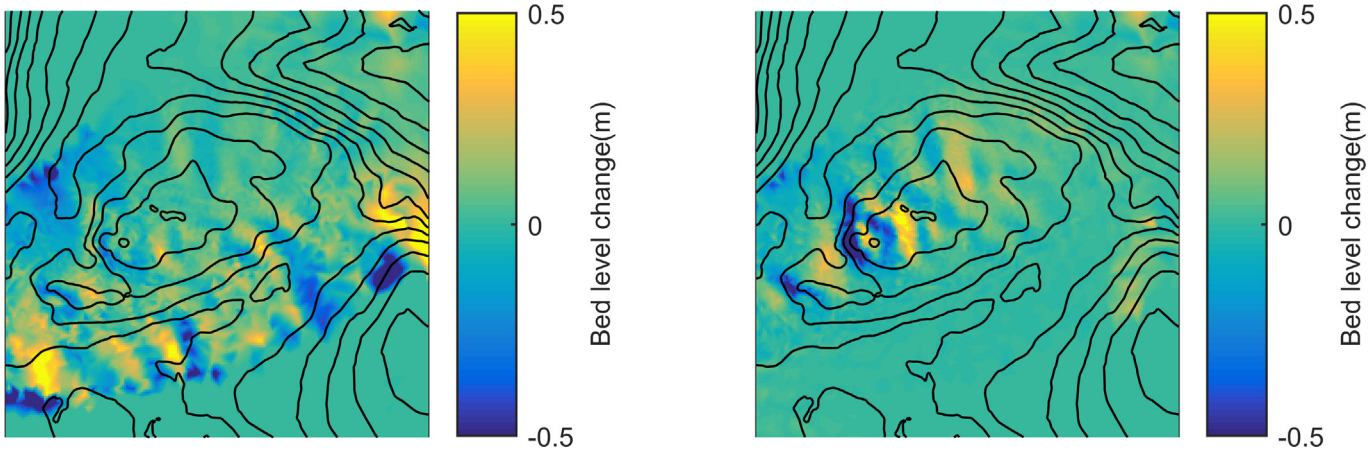

Fig. 19. Bed level changes for the winter case with waves included for (left) the natural case and (right) the energy extraction case. Black lines indicate the bathymetric contours at the start of the simulation. The area shown is a close up of the inner sound sandbank.

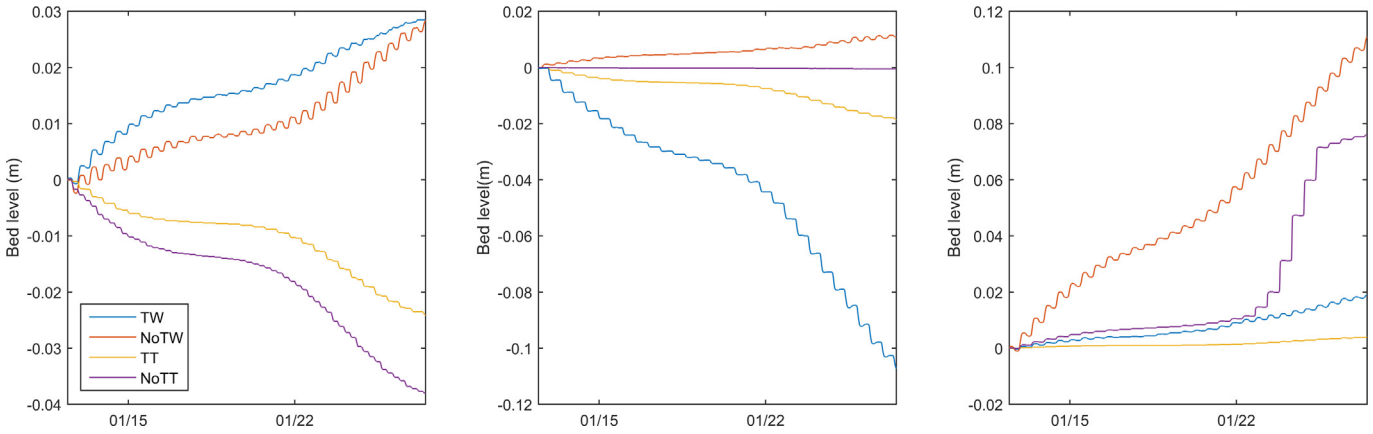

Fig. 20. Bed level changes from the initial bed level for the winter scenarios with turbines and waves (TW), no turbines and waves (NoTW), turbines and tide only (TT) and no turbines tide only (NoTT). Data is plotted for (a) the point on the crest; (b) the point on the NW flank; (c) the point on the SE flank.

Table 2
Volume change, m^3 and % of total volume, for the different scenarios and differences in volume change between the scenarios. Differences caused by turbine implementation are displayed in the right-hand column and differences caused by activation of waves in the simulations given in the third row (summer case) and sixth row (winter case).

	No turbines	Turbines	*Difference in volume change caused by turbine implementation*
Summer tide only	$-778 m^3$ (−0.11%)	$-338 m^3$ (0.05%)	*440* m^3 (0.07%)
Summer, waves and tides	$6198 m^3$ (0.94%)	$7172 m^3$ (1.09%)	*974* m^3 (0.14%)
Difference caused by waves (summer)	*6976* m^3 (1.06%)	*7510* m^3 (1.14%)	*534* m^3 (0.08%)
Winter tide only	$-1680 m^3$ (−0.25%)	$-772 m^3$ (−0.11%)	*908* m^3 (0.14%)
Winter, waves and tides	$8501 m^3$ (1.29%)	$11{,}081 m^3$ (1.68%)	*2580* m^3 (0.39%)
Difference caused by waves (winter)	*10,181* m^3 (1.55%)	*11,853* m^3 (1.80%)	*1672* m^3 (0.25%)

6. Discussion

Inclusion of wave action increases magnitude of sediment transport. Given the minimal changes to the depth averaged hydrodynamics it is believed that this increase is primarily caused by the enhanced mobilisation of sediment caused by the orbital velocities.

Reductions in sandbank volume are predicted for the tide only cases and increases in sandbank volume when waves are activated. This suggests there may be an interplay between periods of calm and periods of wave activity in the long-term stability of the sand bank. Similar interplay has been previously demonstrated by the authors for sand banks in the Bristol Channel [21]. Predicted volumetric changes are up to 1.5% of the sandbank volume. Given that this change is over a two week period this is a significant change. Assumptions of spherical particles are made in the sediment transport calculations. McIlveny et al. [54] found that the majority of particle are plate shaped, hence having lower form drag and greater resistance to motion. This means that sediment transport and morphological change may well be over predicted in an absolute sense. However it is expected that direction of change and sediment transport pathways will still be correctly predicted. Given the comparative nature of this study it is believed that the conclusions are still valid.

This research suggests that for tidal stream sites with energetic wave climates, accurate modelling of impact to morphodynamics may require inclusion of wave action in simulations. Greater changes to baseline conditions are observed when waves are implanted compared to the change when turbines are implemented. Moreover, the change in impact when waves are included is not linear, and hence the contribution to change caused bay waves cannot be simply added to hydrodynamic simulations with and without turbines. The results show the impact of the large sand waves on the sandbank on the predicted patterns of erosion and accretion and these dictate that the patterns of direction of change are similar with and without wave action included.

Inclusion of wave action in modelling leads to increases in computational expense, time needed for model set-up and additional data requirements for boundary forcing and calibration studies. Therefore, the decision to include waves is not a trivial one. The relative importance of waves will depend on the wave exposure of the mobile sediment receptors for a given project. Thus, while wave action should not be ignored, it is recommended that assessment of wave climate in these regions is undertaken prior to the modelling decision.

The numerical model used in this study does not include the influence of waves on apparent bed roughness that is felt by currents. Wave generated turbulence and the interaction of the wave and current boundary layers will increase the apparent roughness felt by the current and hence reduce current speeds. Omission of this physical phenomena means that the effect of waves on tidal stream turbine impact may be under represented.

7. Conclusions

This study has investigated the impact of TST energy extraction on a sub-tidal sandbank in the Inner Sound of the Pentland Firth and focused on whether it is necessary to include waves in the

simulation of TSTs and their impact on morphodynamics.

For the inner sound of the Pentland Firth, inclusion of TSTs at the tested level has minimal impact on the wave field. Since the tested level was at the higher limits of likely extraction, the impact of tidal stream turbines on wave climate is seen as unimportant here.

Inclusion of wave action can alter tidal currents however this alteration largely depends on the wave direction. Minimal differences in tidal current are seen for waves incident from the east whereas a more noticeable difference is observable when waves are incident from the north west. The difference caused by inclusion of waves on turbine impact on hydrodynamics is small, typically less than 5% of the impact predicted without waves. More consistent differences are observed in the predictions of sediment transport. Inclusion of wave action increases magnitude of sediment transport.

The difference in volumetric sea bed change caused by inclusion of waves in the simulation is greater than the difference in volume change caused by inclusion of turbines and hence ignoring waves in simulations is likely to produce erroneous results in terms of magnitudes. However the direction of volumetric change is the same for simulations with and without waves.

These conclusions mean that it is recommended that investigators do not ignore the inclusion of waves in simulations of tidal stream turbines on morphodynamics a priori but rather assess the wave climate of a specific site before making a decision on inclusion of waves. The relative importance will depend on the wave exposure of different sites, the depth of the sandbanks and other environmental factors.

Acknowledgments

This work was financially supported by the UK EPSRC via Terawatt (EP/J010170/1), Ecowatt (EP/K012851/1) and “Extension of UKCMER Core Research, Industry and International Engagement” (EP/M014738/1) projects. We acknowledge the kind provision of the wave data in the Pentland Firth used for model validation by Dr. Philippe Glezion from ERI. Supply of data by the British Geological Society and Marine Scotland Science under licence to the Terawatt consortium is also acknowledged. All data sources are refenced in the text. Model outputs used in this study are made open source at https://doi.org/10.5281/zenodo.1189399.

References

[1] Metoc Aecom, Pentland Firth and Orkney Waters Marine Spatial Plan Framework & Regional Locational Guidance for Marine Energy. Marine Scotland, 2011.
[2] MeyGen, MeyGen Tidal Energy Project - Phase 1: Environmental Statement, 2012.
[3] L.M. Ashall, R.P. Mulligan, B.A. Law, Variability in suspended sediment concentration in the Minas Basin, Bay of Fundy, and implications for changes due to tidal power extraction, Coast. Eng. 107 (2016) 102–115.
[4] I. Masters, A. Williams, T.N. Croft, M. Togneri, M. Edmunds, E. Zangiabadi, I. Fairley, H. Karunarathna, A comparison of numerical modelling techniques for tidal stream turbine analysis, Energies 8 (2015) 7833–7853.
[5] S. Nash, N. O'Brien, A. Olbert, M. Hartnett, Modelling the far field hydro-environmental impacts of tidal farms - a focus on tidal regime, inter-tidal zones and flushing, Comput. Geosci. 71 (2014) 20–27.
[6] V. Ramos, R. Carballo, M. Sanchez, M. Veigas, G. Iglesias, Tidal stream energy impacts on estuarine circulation, Energy Convers. Manag. 80 (2014) 137–149.
[7] Z. Yang, T. Wang, A. Copping, S. Geerlofs, Modeling of in-stream tidal energy development and its potential effects in Tacoma Narrows, Washington, USA, Ocean Coast Manag. 99 (2014) 52–62.
[8] D.S. Busch, C.M. Greene, T.P. Good, Estimating effects of tidal power projects and climate change on threatened and endangered marine species and their food web, Conserv. Biol. 27 (2013) 1190–1200.
[9] A. Copping, H. Battey, J. Brown-Saracino, M. Massaua, C. Smith, An international assessment of the environmental effects of marine energy development, Ocean Coast Manag. 99 (2014) 3–13.
[10] A. Copping, L. Hanna, B. Van Cleve, K. Blake, R.M. Anderson, Environmental risk evaluation system-an approach to ranking risk of ocean energy development on coastal and estuarine environments, Estuar. Coast 38 (2015) S287–S302.
[11] M.K. Pine, A.G. Jeffs, C.A. Radford, The cumulative effect on sound levels from multiple underwater anthropogenic sound sources in shallow coastal waters, J. Appl. Ecol. 51 (2014) 23–30.
[12] A. Berthot, C. Pattiaratchi, Maintenance of headland-associated linear sandbanks: modelling the secondary flows and sediment transport, Ocean Dynam. 55 (2005) 526–540.
[13] A. Berthot, C. Pattiaratchi, Mechanisms for the formation of headland-associated linear sandbanks, Continent. Shelf Res. 26 (2006) 987–1004.
[14] S.P. Neill, The role of Coriolis in sandbank formation due to a headland/island system. Estuarine, Coast. Shelf Sci. 79 (2008) 419–428.
[15] C. Pattiaratchi, M. Collins, Mechanisms for linear sandbank formation and maintenance, in realtion to dynamical oceanographic observations, Prog. Oceanogr. 19 (1987) 117–176.
[16] A. Chatzirodou, H. Karunarathna, Impacts of Tidal Eneryg Extraction on Sea Bed Morphology, ICCE, Seoul, Korea, 2014.
[17] A. Giardino, D. Van den Eynde, J. Monbaliu, Wave effects on the morphodynamic evolution of an offshore sand bank, J. Coast. Res. 51 (2010) 127–140.
[18] J.W.H. van de Meene, L.C. van Rijn, The shoreface-connected ridges along the central Dutch coast - part 1: field observations, Continent. Shelf Res. 20 (2000) 2295–2323.
[19] M.J. Lewis, S.P. Neill, A.J. Elliott, Interannual variability of two offshore sand banks in a region of extreme tidal range, J. Coast. Res. 31 (2) (2014) 265–275.
[20] C.E. Vincent, A. Stolk, C.F.C. Porter, Sand suspension and transport on the Middelkerke Bank (southern North Sea) by storms and tidal currents, Mar. Geol. 150 (1998) 113–129.
[21] I. Fairley, I. Masters, H. Karunarathna, Numerical modelling of storm and surge events on offshore sandbanks, Mar. Geol. 371 (2016) 106–119.
[22] C. Pattiaratchi, M.B. Collins, Wave influence of coastal sand transport paths in a tidally dominated environment, Ocean Shorel. Manag. 11 (1988) 49–465.
[23] R.L. Soulsby, L. Hamm, G. Klopman, D. Myrhaug, R.R. Simons, G.P. Thomas, Wave-current interaction within and outside the bottom boundary layer, Coast. Eng. 21 (1993) 41–69.
[24] J. Wolf, D. Prandle, Some observations of wave-current interaction, Coast. Eng. 37 (1999) 471–485.
[25] L.H. Holthuijsen, Waves in Oceanic and Coastal Waters, Cambridge University Press, 2010.
[26] A. Chawla, J.T. Kirby, Experimental Study of Wave Breaking and Blocking on Opposing Currents, 1999.
[27] A. Chawla, J.T. Kirby, Monochromatic and random wave breaking at blocking points, J. Geophys. Res. 107 (2002).
[28] N. Guillou, G. Chapalain, S.P. Neill, The influence of waves on the tidal kinetic energy resource at a tidal stream energy site, Appl. Energy 180 (2016) 402–415.
[29] M.R. Hashemi, S.P. Neill, P.E. Robins, A.G. Davies, M.J. Lewis, Effect of waves on the tidal energy resource at a planned tidal stream array, Renew. Energy 75 (2015) 626–639.
[30] I. Fairley, R. Ahmadian, R.A. Falconer, M.R. Willis, I. Masters, The effects of a severn barrage on wave conditions in the Bristol Channel, Renew. Energy 68 (2014) 428–442.
[31] A. Chatzirodou, H. Karunarathna, D.E. Reeve, Modelling the Response of Tidal Sandbank Dynamics to Tidal Energy Extraction, IAHR World Congress, The Hague, Netherlands, 2015.
[32] I. Fairley, I. Masters, H. Karunarathna, The cumulative impact of tidal stream turbine arrays on sediment transport in the Pentland Firth, Renew. Energy 80 (2015a) 755–769.
[33] I. Fairley, I. Masters, H. Karunarathna, Sediment transport in the Pentland Firth and impacts of tidal stream energy extraction, in: 11th European Wave and Tidal Energy Conference, Nantes, France, 2015.
[34] R. Martin-Short, J. Hill, S.C. Kramer, A. Avdis, P.A. Allison, M.D. Piggott, Tidal resource extraction in the Pentland Firth, UK: potential impacts on flow regime and sediment transport in the Inner Sound of Stroma, Renew. Energy 76 (2015) 596–607.
[35] S.P. Neill, J.R. Jordan, S.J. Couch, Impact of tidal energy converter (TEC) arrays on the dynamics of headland sand banks, Renew. Energy 37 (2012) 387–397.
[36] S.P. Neill, E.J. Litt, S.J. Couch, A.G. Davies, The impact of tidal stream turbines on large-scale sediment dynamics, Renew. Energy 34 (2009) 2803–2812.
[37] P.E. Robins, M.J. Lewis, S.P. Neill, Impact of tidal-stream arrays in relation to the natural variability of sedimentary processes, Renew. Energy 72 (2014a) 311–321.
[38] P.E. Robins, S.P. Neill, M.J. Lewis, Impacts of Tidal-stream Energy Converter TEC Arrays in Realtion to the Natural Variability of Sedimentary Processes, EIMR2014, Stornoway, Scotland, 2014b.
[39] J. Thiebot, P.B. du Bois, S. Guillou, Numerical modeling of the effect of tidal stream turbines on the hydrodynamics and the sediment transport - application to the Alderney Race (Raz Blanchard), France, Renew. Energy 75 (2015) 356–365.
[40] I. Fairley, H. Karunarathna, Assessing the Importance of Including Waves in Simulations of Tidal Stream Turbine Impacts, RENEW2016, Lisbon, Portugal, 2016.
[41] P.P. Mathisen, O.S. Madsen, Waves and currents over a fixed rippled bed 2. Bottom and apparent roughness experienced by currents in the presence of waves, J. Geophys. Res. 101 (C7) (1996) 16543–16550.
[42] T.A.A. Adcock, S. Draper, G.T. Houlsby, A.G.L. Borthwick, On the tidal resource

of the Pentland Firth, in: 4th International COnference on Ocean Energy, Dublin, 2012.
[43] T.A.A. Adcock, S. Draper, G.T. Houlsby, A.G.L. Borthwick, S. Serhadlioglu, The available power from tidal stream turbines in the Pentland Firth, in: Proceedings of the Royal Society A-Mathematical Physical and Engineering Sciences, 2013, p. 469.
[44] T.A.A. Adcock, S. Draper, G.T. Houlsby, A.G.L. Borthwick, S. Serhadlioglu, Tidal stream power in the Pentland Firth - long-term variability, multiple constituents and capacity factor, Proc. IME J. Power Energy 228 (2014) 854–861.
[45] S. Baston, R.E. Harris, Modelling the hydrodynamic characteristics of tidal flow in the Pentland Firth, in: EWTEC 2011, Southampton, 2011.
[46] S. Draper, T.A.A. Adcock, A.G.L. Borthwick, G.T. Houlsby, Estimate of the tidal stream power resource of the Pentland Firth, Renew. Energy 63 (2014) 650–657.
[47] M.C. Easton, D.K. Woolf, P.A. Bowyer, The dynamics of an energetic tidal channel, the Pentland Firth, Scotland, Continent. Shelf Res. 48 (2012) 50–60.
[48] L. Goddijn-Murphy, D.K. Woolf, M.C. Easton, Current patterns in the inner sound (Pentland Firth) from underway ADCP data, J. Atmos. Ocean. Technol. 30 (2013) 96–111.
[49] G.R. Osborn, C.L. Hinton, W.S. Cooper, Pentland Firth and Orkney Waters Strategic Area: Marine Energy Resources, ABPmer/the Crown Estate, 2012.
[50] A. Saruwatari, D.M. Ingram, L. Cradden, Wave-current interaction effects on marine energy converters, Ocean Eng. 73 (2013) 106–118.
[51] S.P. Neill, M.J. Lewis, M.R. Hashemi, E. Slater, J. Lawrence, S.A. Spall, Inter-annual and inter-seasonal variability of the Orkney wave power resource, Appl. Energy 132 (2014) 339–348.
[52] M.A. Johnson, N. Kenyon, R.H. Belderson, A.H. Stride, Sand transport, in: A.H. Stride (Ed.), Offshore Tidal Sands. Processes and Deposits, Chapman and Hall, 1982, pp. 58–94.
[53] G.E. Farrow, N.H. Allen, E.B. Akpan, Bioclastic carbonate sedimentation on a high latitude, tide-dominated shelf: northeast Orkney Islands, Scotland, J. Sediment. Petrol. 54 (1984) 373–393.
[54] J. McIlvenny, D. Tamsett, P. Gillibrand, L. Goddijn-Murphy, On the sediment dynamics in a tidally energetic channel: the inner sound, northern Scotland, J. Mar. Sci. Eng. 4 (2016).
[55] DHI, MIKE3 Flow Model FM - Sand Transport Module - User Guide, DHI, 2012.
[56] British Geological Survey, BGS legacy particle size analysis uncontrolled data export, in: Dataset Supplied to TeraWatt Project, 2013.
[57] S. Baston, S. Waldman, J. Side, Modelling energy extraction in tidal flows, in: Terawatt Position Papers: a 'toolbox' of Mthods to Better Understand and Asses the Effects of Tidal and Wave Energu Arrays on the Marine Environment, MASTS, 2015, pp. 75–108.
[58] R. O'hara Murray, Tidal stream and wave energy array scenarios for the Pentland Firth and Orkney waters strategic area, in: Terawatt Position Papers: a 'toolbox' of Mthods to Better Understand and Asses the Effects of Tidal and Wave Energu Arrays on the Marine Environment, MASTS, 2015, pp. 31–48.
[59] NTSLF, 2016, website: http://www.ntslf.org/tgi/portinfo?port=Wick.
[60] DHI, MIKE21 and MIKE3 Flow Model FM – Sand Transport Module – Scientific Documentation. DHI, 2017.
[61] J.A. Zyserman, J. Fredsoe, Validation of a Deterministic Sediment Transport Model for Sheet Flow Conditions, Progress Reort 76, Institute of Hydrodyanmics and Hydraulic Engineering. Technical University of Denmark, 1996, pp. 1–7.
[62] K. Hu, P. Ding, Z. Wang, S. Yang, A 2D/3D hydrodynamic and sediment transport model for the Yangtze Estuary, China, J. Mar. Syst. 77 (1–2) (2009) 114–136.
[63] M. Sedigh, R. Tomlinson, N. Cartwright, A. Etemad-Shahidi, Numerical simulation of the morphodynamics of the gold coast seaway, in: 21st International Congress on Modelling and Simulation (MODSIM), 2015, pp. 1247–1253.
[64] O. Stocheck, C. Zimmermann, Water exchange and sedimentation in an estuarine tidal harbor using three-dimensional simulation journal of waterway, port, Coast. Ocean Eng. 132 (5) (2006).